



Design of joint differential for transformation of two rotary movements to linear motion.

Master Thesis

Study programme: N2301 Mechanical Engineering
Study branch: Machines and Equipment Design

Author: **Ramlal Gujuluva Ravindran**
Thesis Supervisors: Ing. Šimon Kovář, Ph.D.
Department of Design of Textile Machine





Master Thesis Assignment Form

Design of joint differential for transformation of two rotary movements to linear motion.

Name and surname: **Ramlal Gujuluva Ravindran**
Identification number: S18000458
Study programme: N2301 Mechanical Engineering
Study branch: Machines and Equipment Design
Assigning department: Department of Design of Textile Machine
Academic year: **2019/2020**

Rules for Elaboration:

1. Perform differential mechanisms research.
2. Design at least two variants of kinematic chain for given parameters. The kinematic chain will contain two electronically controlled rotary drives. The driven member will perform a linear reciprocating motion that can be continuously changed.
3. Select a better variant.
4. Create CAD documentation for the select variant.

Scope of Graphic Work: CAD documentation
Scope of Report: 35 A4 pages
Thesis Form: printed/electronic
Thesis Language: English



List of Specialised Literature:

1. AMBEKAR, Ashok G. *Mechanism and machine theory*. Delhi: PHI Learning Private Limited, [2007]. Eastern economy. ISBN 978-81-203-3134-1.
2. RAO, J. S. a Rao V. DUKKIPATI. *Mechanism and machine theory*. Second edition. New Delhi: New Age International (p) Limited Publishers, 1992. ISBN 81-224-0426-X.
3. NORTON, Robert L. *Design of machinery: an introduction to the synthesis and analysis of mechanisms and machines*. Fifth edition. New York: McGraw-Hill, [2012]. McGraw-Hill series in mechanical engineering. ISBN 978-0-07-352935-6.
4. MEERKAMM, Harald. Technical pocket guide. University of Erlangen-Nuremberg. Schaeffler Technologies GmbH & Co.KG, 1st edition, March 2014. MATNR 084713119

Thesis Supervisors: Ing. Šimon Kovář, Ph.D.
Department of Design of Textile Machine

Date of Thesis Assignment: October 30, 2019

Date of Thesis Submission: January 31, 2022

prof. Dr. Ing. Petr Lenfeld
Dean

L.S.

doc. Ing. Martin Bílek, Ph.D.
Head of Department

Liberec October 30, 2019

Declaration

I hereby certify, I, myself, have written my master thesis as an original and primary work using the literature listed below and consulting it with my thesis supervisor and my thesis counsellor.

I acknowledge that my bachelor master thesis is fully governed by Act No. 121/2000 Coll., the Copyright Act, in particular Article 60 – School Work.

I acknowledge that the Technical University of Liberec does not infringe my copyrights by using my master thesis for internal purposes of the Technical University of Liberec.

I am aware of my obligation to inform the Technical University of Liberec on having used or granted license to use the results of my master thesis; in such a case the Technical University of Liberec may require reimbursement of the costs incurred for creating the result up to their actual amount.

At the same time, I honestly declare that the text of the printed version of my master thesis is identical with the text of the electronic version uploaded into the IS/STAG.

I acknowledge that the Technical University of Liberec will make my master thesis public in accordance with paragraph 47b of Act No. 111/1998 Coll., on Higher Education Institutions and on Amendment to Other Acts (the Higher Education Act), as amended.

I am aware of the consequences which may under the Higher Education Act result from a breach of this declaration.

May 28, 2021

Ramlal Gujuluva Ravindran

ACKNOWLEDGEMENT

I would like to express my deepest gratitude to my thesis professor **Ing. Šimon Kovář, Ph.D.**, for his guidance, giving me expert advises and dedicating his precious time for making this thesis possible. Thanks a lot for the knowledge you provided which kept me learning many new things and making this thesis better.

I would like to thank doc. Ing. Martin Bílek Ph.D., prof. Ing. Jaroslav Beran CSc., Ing. Petr Žabka Ph.D., Ing. Jan Valtera Ph.D., Ing. Jiří Komárek Ph.D., Ing. Martin Konečný Ph.D. for your expert guidance and helping me to complete my course.

I would like to thank **Technical University of Liberec** for providing me beautiful experience and learn new things in my life.

I would like to thank **my parents and family members** for providing me this great opportunity to study at the TUL and supporting me throughout the studies.

I would also like to thank **my friends** who have been supportive and making it a fun throughout the course of study.

ABSTRACT

This thesis aims to design a differential linkage mechanism that provides a range of stroke variation. Research done and different variants are proposed. The 3D model of differential mechanism built in PTC creo parametric system. It is a seven bar mechanism which requires two drives for its operation. Kinematic analysis done for determining the dimension of the links in the model and the required output achieved so that different values of stroke variation is possible from single mechanism. Dynamic analysis done using PTC creo parametric mechanism for analysing forces at their joints. Stress analysis done using PTC creo parametric simulation for observing the stress and displacement behaviour of the mechanism. CAD documentation of final model done and reviewed.

Keywords

Differential mechanism, Eccentric, Link, Stroke variation, Bearing, Radial force.

ABSTRAKT

Tato práce si klade za cíl navrhnout mechanismus diferenciálního propojení, který poskytuje řadu variací zdvihu. Je proveden výzkum a jsou navrženy různé varianty. 3D model diferenciálního mechanismu zabudovaného v PTC kreio parametrickém systému. Jedná se o sedmibodový mechanismus, který ke svému provozu vyžaduje dva pohony. Byla provedena kinematická analýza pro určení dimenze vazeb v modelu a požadovaný výstup, takže z jednoho mechanismu jsou možné různé hodnoty variace zdvihu. Dynamická analýza prováděná pomocí PTC parametrického mechanismu pro analýzu sil v jejich spojích. Analýza napětí pomocí PTC kreio parametrické simulace pro sledování chování mechanismu napětí a posunutí. CAD dokumentace finálního modelu hotová a zkontrolovaná.

klíčová slova

Diferenciální mechanismus, excentrický, článek, variace zdvihu, ložisko, radiální síla.

CONTENTS

1	INTRODUCTION	15
1.1	Scope	15
1.2	Aim.....	15
2	LITERATURE REVIEW	16
2.1	Kinematics.....	16
2.2	Dynamics.....	16
2.3	Mechanism	16
2.4	Classification of links.....	16
2.4.1	Binary link	16
2.4.2	Ternary link.....	17
2.4.3	Quaternary link	17
2.5	Kinematic pair	17
2.5.1	Classification of kinematic pair	17
2.6	Realisation of joints.....	18
2.6.1	2D.....	18
2.6.2	3D.....	19
2.7	Kinematic chain.....	20
2.8	Degrees of freedom (i)	21
2.8.1	2D.....	21
2.8.2	3D.....	21
2.9	Transfer function	21
2.10	Transmission angle	22
2.11	Selection of bearing for the mechanism	23
2.11.1	Reduce friction and allow turn more smooth.....	24
2.11.2	Supports and maintain shaft position during rotation	24
2.12	Selection of material for the mechanism building	24
3	SEVEN BAR MECHANISM	24
3.1	Line model.....	24
3.2	Building of mechanism	25
3.2.1	Recommendation of length of links	26
3.2.2	Equations of mechanism	26
3.3	Selection of ground for second Eccentric	28
4	DESIGN PROPOSAL	29
4.1	Requirement of mechanism.....	29
4.2	Variant-1.....	29
4.3	Variant-2.....	29

5	PROPOSED VARIANT	30
5.1	Version-1	30
5.1.1	Initial structure	30
5.1.2	Analysis of stroke variation for initial structure	31
5.1.3	Modified structure.....	33
5.1.4	Final structure of version-1	36
5.1.5	Analysis of radial forces of version-1	36
5.1.6	Bearing selection.....	38
5.2	Version-2.....	38
5.2.1	Building of mechanism	38
5.2.2	Dimension of eccentrics.....	41
5.2.3	Optimization of slider axis.....	44
6	BUILDING OF REAL MODEL	46
6.1	Design of links	46
6.1.1	Eccentric shaft 1.....	46
6.1.2	Eccentric shaft 2.....	46
6.1.3	Ternary link.....	47
6.1.4	Connecting rod 1.....	47
6.1.5	Connecting rod 2.....	48
6.1.6	Slider joint.....	48
6.2	Selection of slider.....	49
6.3	Selection of bearing.....	49
6.3.1	Radial force at eccentric 1 (A_oA) in x direction	50
6.3.2	Radial force at eccentric 1 (A_oA) in y direction	50
6.3.3	Radial force at eccentric 2 (D_oD) in x direction.....	51
6.3.4	Radial force at eccentric 2 (D_oD) in y direction.....	51
6.3.5	Radial force at joint B in x direction.....	52
6.3.6	Radial force at joint B in y direction.....	52
6.3.7	Radial force at joint C in x direction.....	53
6.3.8	Radial force at joint C in y direction.....	53
6.3.9	Radial force at joint E in x direction.....	54
6.3.10	Radial force at joint E in y direction.....	54
6.3.11	Type of bearing selected	55
6.4	Model assembly.....	56
6.5	Stress analysis	57
6.5.1	Analysis of eccentric A_oA	57
6.5.2	Analysis of eccentric D_oD	58



6.5.3	Analysis of link ₁	59
6.5.4	Analysis of link ₂	60
6.5.5	Analysis of link ₃	61
7	CONCLUSION.....	62
8	REFERENCES	63

LIST OF FIGURES

Figure 2.1: Binary link	16
Figure 2.2: Ternary link	17
Figure 2.3: Quaternary link	17
Figure 2.4: Pin joint	18
Figure 2.5: Slider joint	19
Figure 2.6: Screw joint.....	19
Figure 2.7: Cylindrical joint.....	19
Figure 2.8: Planar joint	20
Figure 2.9: Spherical joint.....	20
Figure 2.10: Simple Four bar mechanism.....	20
Figure 2.11: Four bar mechanism describing transfer function.....	22
Figure 2.12: Slider crank mechanism describing transfer function	22
Figure 2.13: Slider crank mechanism describing transmission angle.....	23
Figure 3.1: Line model of seven-bar mechanism.....	25
Figure 3.2: Triangle formed by points A, B, C	26
Figure 3.3: Triangle formed by Eccentric A_0A	27
Figure 3.4 Triangle formed by Eccentric C_0C	27
Figure 3.5: Selection of ground from first dead centre	28
Figure 3.6: Selection of ground from second dead centre	28
Figure 4.1: Line diagram for the variant-1.....	29
Figure 4.2: Line diagram for the variant-2.....	29
Figure 5.1: Line model of initial structure	30
Figure 5.2: Line model showing eccentric angles	31
Figure 5.3: Stroke variation when length of both eccentrics are 5 mm	32
Figure 5.4: Stroke variation when length of both eccentrics are 8 mm	32
Figure 5.5: Line model of modified structure	33
Figure 5.6: Stroke variation for different combination of eccentric lengths.....	34
Figure 5.7: Stroke variation for selected eccentric lengths.....	35
Figure 5.8: Final structure of version-1	36
Figure 5.9: Radial force at joint A	36
Figure 5.10: Radial force at joint B	37
Figure 5.11: Radial force at joint C	37
Figure 5.12: Line diagram of version-2	38
Figure 5.13: Triangle formed by points A, B, C.....	39
Figure 5.14: Triangle formed by eccentric A_0A	40
Figure 5.15: Triangle formed by points A, C, D.....	40
Figure 5.16: Triangle formed by eccentric D_0D	41
Figure 5.17: Stroke variation for different values of eccentrics	42
Figure 5.18: Stroke variation for chosen eccentrics.....	43
Figure 5.19: Displacement of slider axis to the eccentric 1 axis	44
Figure 5.20: Stroke variation for slider axis displacement	44
Figure 5.21: Stroke variation when slider displaced by 7.5 mm	45
Figure 6.1: Eccentric shaft 1	46
Figure 6.2: Eccentric shaft 2	46
Figure 6.3: Ternary link	47
Figure 6.4: Connecting rod 1	47
Figure 6.5: Connecting rod 2	48



Figure 6.6: Slider joint	48
Figure 6.7: Linear guide.....	49
Figure 6.8: Line diagram of version-2	49
Figure 6.9: Radial force at eccentric1 (A_oA) in X direction	50
Figure 6.10: Radial force at eccentric 1 (A_oA) in Y direction	50
Figure 6.11: Radial force at eccentric 2 (D_oD) in x direction	51
Figure 6.12: Radial force at eccentric 2 (D_oD) in y direction	51
Figure 6.13: Radial force at joint B in x direction	52
Figure 6.14: Radial force at joint B in y direction	52
Figure 6.15: Radial force at joint C in x direction	53
Figure 6.16: Radial force at joint C in y direction	53
Figure 6.17: Radial force at joint E in x direction	54
Figure 6.18: Radial force at joint E in y direction	54
Figure 6.19: GBB flanged plain bearing.....	55
Figure 6.20: SKF needle roller bearing.....	55
Figure 6.21: Model assembly.....	56
Figure 6.22: Stress analysis of eccentric A_oA	57
Figure 6.23: Displacement analysis of eccentric A_oA	57
Figure 6.24: Stress analysis of eccentric D_oD	58
Figure 6.25: Displacement analysis of eccentric D_oD	58
Figure 6.26: Stress analysis of link ₁	59
Figure 6.27: Displacement analysis of link ₁	59
Figure 6.28: Stress analysis of link ₂	60
Figure 6.29: Displacement analysis of link ₂	60
Figure 6.30: Stress analysis of link ₃	61
Figure 6.31: Displacement analysis of link ₃	61

LIST OF TABLES

Table 5.1: Comparison of stroke variation for different eccentric lengths	33
Table 5.2: Stroke variation for selected eccentric lengths	35
Table 5.3: Comparison of radial forces across joints.....	38
Table 5.4: Stroke variation for different values of eccentrics.....	42
Table 5.5: Stroke variation for chosen eccentrics	43
Table 5.6: Stroke variation when slider displaced by 7.5 mm.....	45
Table 6.1: Maximum force at joints.....	55
Table 6.2: Maximum load of friction bearing.....	55
Table 6.3: Maximum force at eccentrics.....	56
Table 6.4: Maximum load of needle roller bearing	56

LIST OF EQUATIONS

Equation 2.1: Equation of degrees of freedom of a 2D planar kinematic chain	21
Equation 2.2: Equation of degrees of freedom of a 3D spatial kinematic chain	21
Equation 2.3: Transfer function of a four bar mechanism	21
Equation 2.4: Transfer function of slider eccentric mechanism	22
Equation 3.1: Condition to satisfy slider mobility	25
Equation 3.2: Equation to calculate coordinate of point B in x direction.....	26
Equation 3.3: Equation to calculate δ	27
Equation 3.4: Equation to calculate AC.....	27
Equation 3.5: Equation to calculate α	27
Equation 3.6: Equation to calculate ϵ	27
Equation 3.7: Equation to calculate coordinate of point A in x direction.....	27
Equation 3.8: Equation to calculate coordinate of point A in y direction.....	27
Equation 3.9: Equation to calculate coordinate of point C in x direction.....	28
Equation 3.10: Equation to calculate coordinate of point C in y direction.....	28
Equation 3.11: Equation to calculate coordinate of point B in x direction.....	28
Equation 5.1: Equation to satisfy slider mobility.....	31
Equation 5.2: Equation to satisfy slider mobility.....	34
Equation 5.3: Equation to satisfy slider mobility.....	39
Equation 5.4: Equation to calculate coordinate of point B in x direction.....	39
Equation 5.5: Equation to calculate δ	39
Equation 5.6: Equation to calculate α	40
Equation 5.7: Equation to calculate ϵ	40
Equation 5.8: Equation to calculate coordinate of point A in x direction.....	40
Equation 5.9: Equation to calculate coordinate of point A in y direction.....	40
Equation 5.10: Equation to calculate coordinate of point C in x direction.....	40
Equation 5.11: Equation to calculate coordinate of point C in y direction.....	40
Equation 5.12: Equation to calculate δ	41
Equation 5.13: Equation to calculate α	41
Equation 5.14: Equation to calculate ϵ	41
Equation 5.15: Equation to calculate point D in x direction.....	41
Equation 5.16: Equation to calculate point D in y direction.....	41
Equation 5.17: Equation to calculate point B in x direction	41

LIST OF SYMBOLS

- i - Number of degrees of freedom
- n - Number of links
- j - Number of kinematic pairs
- f - Joint's freedom
- μ - Transmission angle (degrees)
- φ_2 - First eccentric angle (degrees)
- φ_5 - Second eccentric angle (degrees)
- e - Slider eccentricity (mm)

1 INTRODUCTION

Mechanism can be found in variety of machines from hand tools to complex machines i.e., from consumer goods likes toys or cameras, scissors, internal combustion engines to aircrafts. Difference between a machine and a mechanism is that all machines can accomplish work, mechanism designed to transform movements into desired set of output forces or moments. For some applications where we might need reciprocating motion output to perform specific task. The rotating input motion of the drive converted into the translating linear motion and the task performed, like in application of shaping machine. [1]

1.1 Scope

In this context, we study about designing of joint differential for transforming of two rotary movements of two drives and producing one linear motion, which sometimes termed as differential mechanism. Numerous mechanical applications conceivably utilized as differential mechanisms i.e., some of them utilized for cutting, printing and pressing. These mechanisms seen in five-bar slider eccentric, seven-bar also in nine bar. Two unique actuators joined with a mechanism to give it a programmable movement. The main aim behind this differential mechanism is that we get rapidly changing slider stroke length, which is dependent upon the angle of difference between the incident angles of each eccentric with respect to common ground. [2]

In spite of many varieties of slider eccentric mechanism, this differential mechanism enables us to provide different slider stroke length without change of dimension of any of the links. Two drives operated using servo drive and programmed for having control over their positions. Therefore, the angle of incident of its corresponding link with the ground can be altered using program.

1.2 Aim

The aim of the thesis is to determine the length of each links analytically and apply the same functionally to demonstrate the variation of stroke length upon range of angle of difference between both incident angles of eccentrics.

The work structure includes the following steps

- Perform research of mechanism and get knowledge about their function and basic building.
- Proposal of two variants of mechanism to perform a linear reciprocating motion whose stroke length changed continuously.
- Analytically determine the length of links and their positions with respect to ground points.
- Select the better variant suitable for the function.
- Design and building of differential mechanism in PTC creo parametric system.
- Create CAD documentation for the design.

2 LITERATURE REVIEW

Understanding the basic function of kinematics and mechanism is very much necessary for the innovation and improvement of new proposals. The following basic principles studied before proceeding to the proposals.

2.1 Kinematics

It is subdivision of theory of machines and it is study of motion. It describes the motion of the body without considering the force that causes the move. It is study of motion of the body in terms of change in distance, velocity or acceleration with respect to time. [3]

2.2 Dynamics

It is subdivision of theory of machines and it is combination of kinematics and kinetics. It is study of motion of the body with respect to force acting on it and masses of the body. [3]

2.3 Mechanism

A mechanism is an arrangement of causally mating parts and cycles that produce one or more motions. They are mechanical function of a machine used to complete a work. They transfer power and motion from one form to another (e.g., rotational to transitional or vice-versa). When a mechanism has four links known as simple mechanism and when a mechanism has more than four links known as compound mechanism. They are assembly of links (rigid, elastic or flexible) connected together by linkage (joints). [3]

2.4 Classification of links

Links are parts of the mechanism and considered as rigid bodies, which connects with another link to drive the mechanism. There are also elastic parts used for transferring motion such as springs but not considered as rigid and so they are not links. They do not affect the kinematics of a mechanism and therefore usually ignored during kinematic analysis. Since they provide motion, considered during the dynamic analysis of mechanism. [3]

The following are the basic classification of links.

2.4.1 Binary link

When one link connected with two more links called binary link. They are connected using revolute or pin joints. The following picture shows an example of binary link.

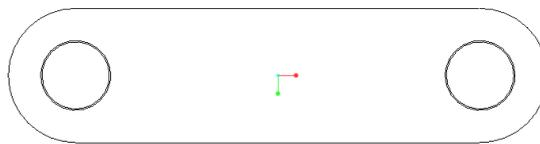


Figure 2.1: Binary link

2.4.2 Ternary link

When one link connected with three more links called ternary link. The following picture shows an example of ternary link.

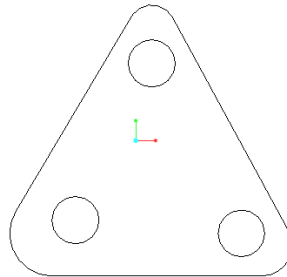


Figure 2.2: Ternary link

2.4.3 Quaternary link

When one link connected with four more links called quaternary link. The following picture shows an example of quaternary link.

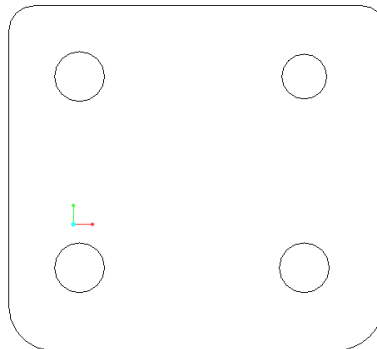


Figure 2.3: Quaternary link

2.5 Kinematic pair

When two links connected with a joint that imposes constraints on relative motion between each other said as a kinematic pair. [3]

2.5.1 Classification of kinematic pair

Classification done under few considerations. The following are the basic classification of kinematic pair.

2.5.1.1 Based on Degrees of freedom

When two bodies are joined, a kinematic pair is formed in which one of the body (base) has all degrees of freedom but the other gets restricted with constraints and has few degrees of freedom relative to the base. Depending on the allowed and constrained degrees of freedom, classified as follows

- 2D
 - Revolute pin joint
 - Slider joint
 - Screw joint

- 3D
 - Cylindrical joint
 - Planar joint
 - Spherical joint

2.5.1.2 Based on Nature of contact

According to the nature of contact between two links of the pair, classified as lower pairs and higher pairs. When two bodies have surface-to-surface contact then they are lower pairs. When two bodies have point or line contact then they are higher pairs.

2.5.1.3 Based on type of closure

According to the way both links joined to have continuous contact, classified as below

- Form closure: The shape of the links joins two links together. Dismantling is difficult.
- Force closure: Contact between both the links are maintained by means of external force i.e., gravity force or spring force or any other means. Dismantling done easily.

2.5.1.4 Based on order of joints

According to the number of links joined, we can classify orders. Order is number of links minus one. Then pin joint between two links is first order pin joint having one degrees of freedom and pin joint between three links is second order pin joint having two degrees of freedom.

2.6 Realisation of joints

In this context, it discusses about how the joints are realised with the links and characterised according to their type.

2.6.1 2D

The following shows the types of joints realised in their 2D space.

2.6.1.1 Pin joint

In mechanical engineering, there are different techniques for fastening objects together. A pin joint is a strong part, like a bolt, which utilizes to interface objects at the connection. This sort of joint permits each object to turn at the point of joint connection. It has one degree of freedom in a mechanism. The following picture shows an example of pin joint.

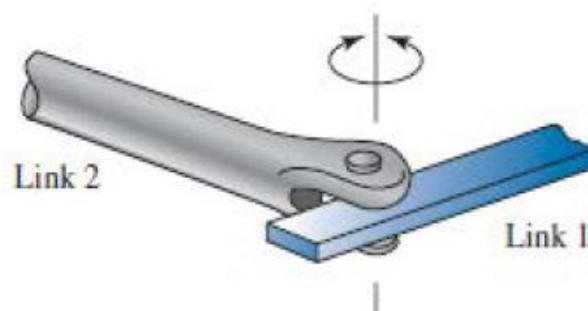


Figure 2.4: Pin joint

2.6.1.2 Slider joint

A Slider joint connects two links allowing only relative motion along a single axis between them. It prevents motion, which is perpendicular to its axis of travel. It has one degree of freedom in a mechanism. The following picture shows an example of slider joint.

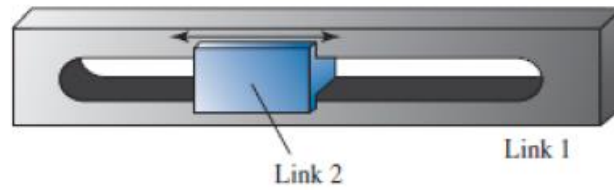


Figure 2.5: Slider joint

2.6.1.3 Screw joint

It is a type of connection used in threaded bolt and nut to travel along single axis between them. They provide translation in most kinds of linear actuators. It has one degree of freedom in a mechanism. The following picture shows an example of screw joint.

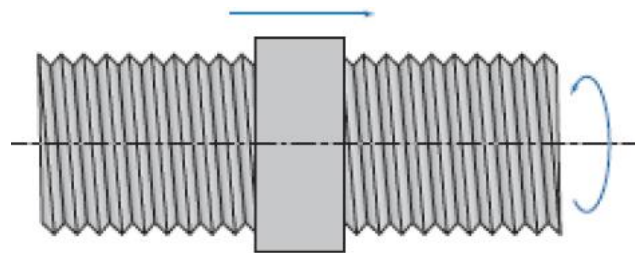


Figure 2.6: Screw joint

2.6.2 3D

The following shows the types of joints realised in their 3D space.

2.6.2.1 Cylindrical joint

It is a type of joint, which has both rotational movement about the cylinder axis and translational movement along the cylinder axis. It is a lower kinematic pair with surface contact and has two degrees of freedom in a mechanism. The following picture shows an example of cylindrical joint.

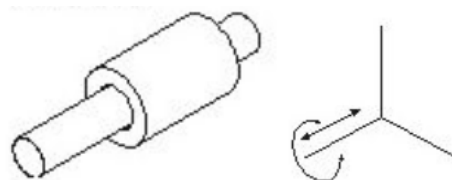


Figure 2.7: Cylindrical joint

2.6.2.2 Planar joint

It has translational movement along the plane in both sides and rotational movement about the axis perpendicular to it. It has two degrees of freedom in a mechanism. The following picture shows an example of planar joint.

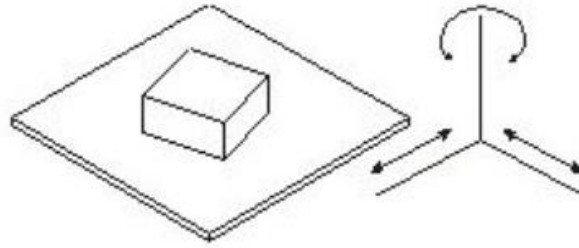


Figure 2.8: Planar joint

2.6.2.3 Spherical joint

It is a kind of ball and socket joint, which allows it to rotate in three degrees. It has three degrees of freedom in a mechanism. The following picture shows an example of spherical joint.

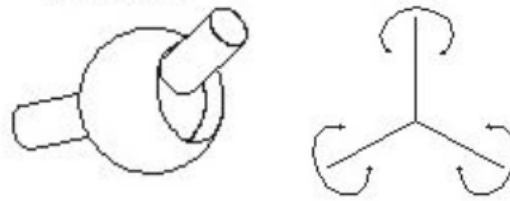


Figure 2.9: Spherical joint

2.7 Kinematic chain

Kinematic chain formed by connecting several number of links with kinematic pairs that has definite relative motion between various links. They can be,

- Open or closed
- Simple or composite
- Free or fixed
- Planar or spatial

To explain in more details, consider an example of simplest kinematic chain which is a four bar chain. Generally, there are four types of four bar mechanism. The following picture shows an example of four bar mechanism.

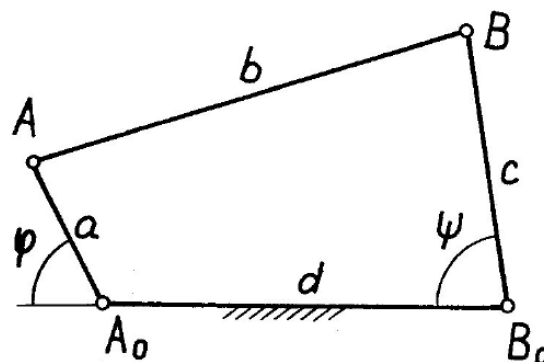


Figure 2.10: Simple Four bar mechanism

It comprises of four links, every one of them forms a turning pair at A_0 , A , B and B_0 . The four links might be of various lengths. according to Grashof's law for a four bar mechanism, the sum of the shortest and, longest link lengths should not be more than the sum of the two remaining link lengths if there is to be persistent relative movement between the two links.

A significant thought in designing a mechanism is to guarantee that the input eccentric makes a complete rotation relative to the other links. The mechanism in which no link makes a complete rotation will not be valuable. In a four bar chain, one of the link, specifically the shortest link, will make a complete rotation relative to the other three links, in the event that it fulfils the Grashof's law, such a link known as eccentric or driver. Link A_0A is an eccentric. The link B_0B that makes a partial rotation or oscillates known as rocker and the link AB that connects the eccentric and rocker called connecting rod. The fixed link A_0B_0 known as frame of the mechanism. At the point when the eccentric is the driver, the mechanism is transforming turning movement into oscillating movement. [3]

2.8 Degrees of freedom (i)

It is the maximum number of individual values required to calculate its final position in space. It defines number of drives required for the mechanism to function. Degrees of freedom of a body in space are six (three translational and three rotational). Degrees of freedom of a body in plane are three (two translational and one rotational). [4]

Let 'i' be number of degrees of freedom, 'n' be number of links, 'j' be number of kinematic pairs and 'f' be joint's freedom. By Grubler's rule, degrees of freedom of a planar kinematic chain is,

2.8.1 2D

The following equations describes the degrees of freedom for a 2D planar kinematic chain. [5]

Equation 2.1: Equation of degrees of freedom of a 2D planar kinematic chain

$$i = 3(n - 1 - j) + \sum_{i=1}^j f_i$$

2.8.2 3D

The following equations describes the degrees of freedom for a 3D spatial kinematic chain. [5]

Equation 2.2: Equation of degrees of freedom of a 3D spatial kinematic chain

$$i = 6(n - 1 - j) + \sum_{i=1}^j f_i$$

2.9 Transfer function

When a system of bodies moves relative to other links i.e., for a one degree of freedom in a four bar mechanism, when an eccentric move, it makes other three links to move relatively. Therefore, when angle φ moves, then there is relative movement of other links or angle ψ . The transfer of movement from one link to other link expressed in terms of geometrical function, called Transfer (kinematic) function. The following equation and picture shows an example of transfer function of a four bar mechanism. [6]

Equation 2.3: Transfer function of a four bar mechanism

$$\Psi = F(a, b, c, d, \varphi)$$

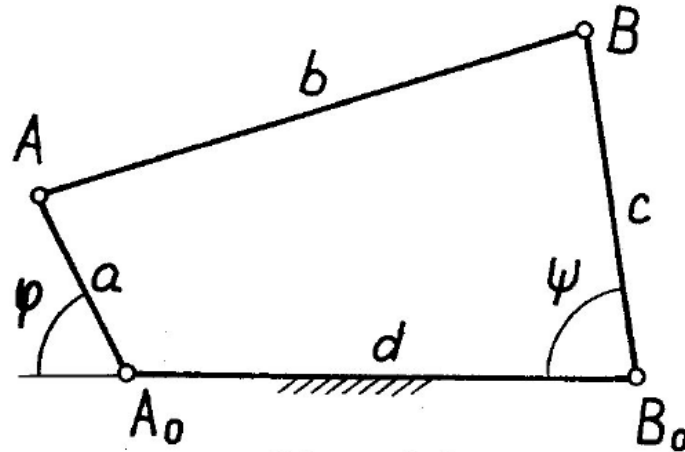


Figure 2.11: Four bar mechanism describing transfer function

In a slider crank mechanism, length of links is constant and angle of crank φ keeps changing to get the desired movement of slider in terms of S . Therefore, we can express function of mechanism in terms of geometrical function called transfer function. The following equation and picture shows an example of transfer function of a slider crank mechanism.

Equation 2.4: Transfer function of slider eccentric mechanism

$$S = F(r, l, \varphi)$$

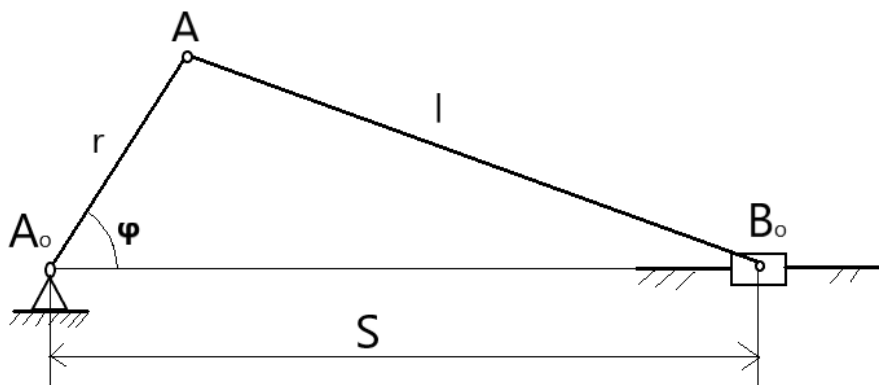


Figure 2.12: Slider crank mechanism describing transfer function

2.10 Transmission angle

It is the angle between coupling link and output link of a mechanism. In other words, angle between the direction of absolute motion (motion with respect to fixed frame) and direction of relative motion (motion with respect to moving frame) of the point at which the output link gets the motion impulse. Used to analyse the quality of the motion transmission in a mechanism. [7]

The optimum angle of transmission angle is 90° . During the motion of mechanism, this angle keeps changing. Depending upon the type of application, this deviation will be around 40° or 50° and even sometimes 70° , in some cases this deviation should be around 20° . When this deviation crosses its critical level, the mechanism will lock. Therefore, if we are not sure of the limit of this deviation, one must consider giving deviation of $\pm 45^\circ$ degree. From the following

picture shows an example of a slider-crank mechanism where letter μ denotes the transmission angle of a slider-crank mechanism.

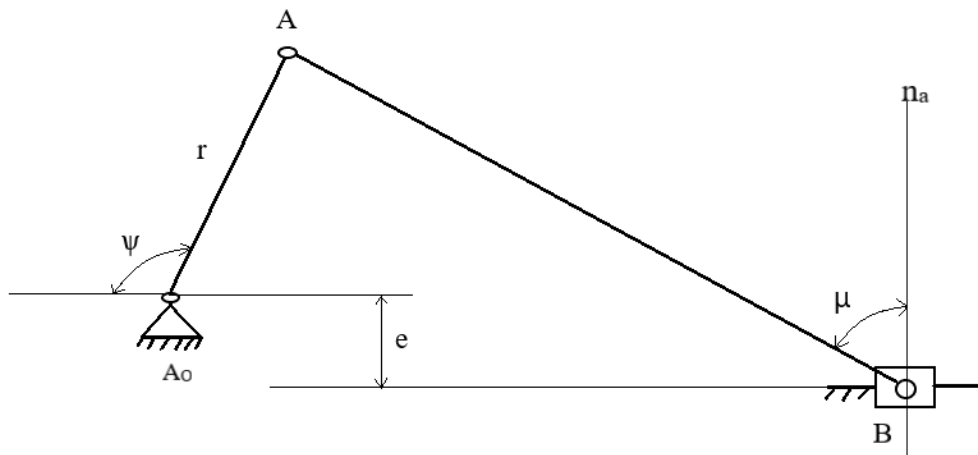


Figure 2.13: Slider crank mechanism describing transmission angle

2.11 Selection of bearing for the mechanism

Bearings are kind of mechanical part. They are utilised in a wide range of machines, they are elements for realizing a kinematic rotating, cylindrical or spherical kinematic pair. They support shaft in a machine to run more smoothly and easily. Thus, for a wide range of machines requires a large number of shafts to operate, hence bearings are utilised always. The fundamental reason for bearing is to avoid direct metal-to-metal contact between two components that are in relative movement. This avoids friction, heat generation and at last, the wear and tear of parts. It additionally decreases energy utilization as sliding movement supplanted with low friction rolling. They additionally transmit the power of the rotating component to the housing. This power might be radial, axial, or a blend of both. A bearing additionally limits freedom of movement of moving parts to predefined directions as said above. The choice of sorting of bearing in a specific application relies on the prerequisite of the application and the attributes of various kinds of course, the rules for choosing an appropriate kind of bearing are as per the following. [8]

- Roller bearings are used for large shaft diameter and heavy load, ball bearings are used for low and medium radial loads
- Self-aligning ball bearings and spherical roller bearings used in place where there will be misalignment between axes of shaft and housing probably going to exist.
- Thrust ball bearings used for medium thrust loads and for heavy thrust loads; cylindrical roller thrust bearings are suggested. There are also double acting thrust bearings, which can convey the thrust load in either direction.
- Deep groove ball bearings, angular contact bearings and spherical roller bearings are appropriate in application where both radial and thrust load acting on bearing components.
- For high-speed application, the maximum allowable speed depends upon the temperature characteristics of bearings. In such high-speed applications, deep groove ball bearings, angular contact bearings and cylindrical roller bearings are suitable.



- In some applications rigidity of bearings are required like in machine tool spindles. Double row cylindrical roller bearings or taper roller bearings used for those conditions. The type of contact of these bearings with application will be line of contact, which improves rigidity of the system.
- Certain places noise becomes the main criteria in application like household appliances. For those applications, deep groove ball bearings used.

Information of the design constraints of different types of bearings and appropriate enthusiasm of the need of an application enables the designer to choose a proper type of bearing. The characteristic of the bearings should match with the necessities of the applications. The following are the important functions of bearings. [9]

2.11.1 Reduce friction and allow turn more smooth

Friction will undoubtedly happen between the rotating shaft and the part that supports the Revolution. Bearings utilized between these two parts. Bearings serve to diminish friction and take into account smoother rotation. This eliminates the measure of energy utilization. This is the absolute most significant capacity of bearings. [8]

2.11.2 Supports and maintain shaft position during rotation

A lot of power is required between the rotating shaft and the part that supports the turn. Bearings play out the capacity of avoiding harm from being finished by this power to the part that supports the rotation, and furthermore of maintaining the right position of the turning shaft. [8]

2.12 Selection of material for the mechanism building

Choice of material is very important for the best mechanical behaviour of mechanism such that suitable to all environment. Steel chosen as the building material for all parts of mechanism. Among steel, E335 is best suitable for our mechanism and the same selected since it is good for both static and dynamic stresses and comparing other parameters.

3 SEVEN BAR MECHANISM

A seven bar mechanism has two degrees of freedom. Therefore, we need two individual drives to operate this mechanism. This kind of mechanism is useful for producing different slider motion during the rotation of two drives. The variable slider motion is achieved when the phase difference between both the eccentric changes.

In this context, we have built a seven bar mechanism in which both the eccentrics are driven by individual servo drive and forms kind of a differential mechanism. When these eccentrics set at an initial angle, they produce an initial slider travel. However, when these eccentrics made to function with different phase difference between their eccentric angles, the resultant slider travel distance varies accordingly. The following content includes the line model of proposal, then determining the dimension of all links of the mechanism. Analysing the slider variation to the different phase difference between both the eccentrics and then building into the working model.

3.1 Line model

For the building of mechanism, a line model made as a first step. The following picture shows the line model made initially for the proposal from a journal reference. [10]

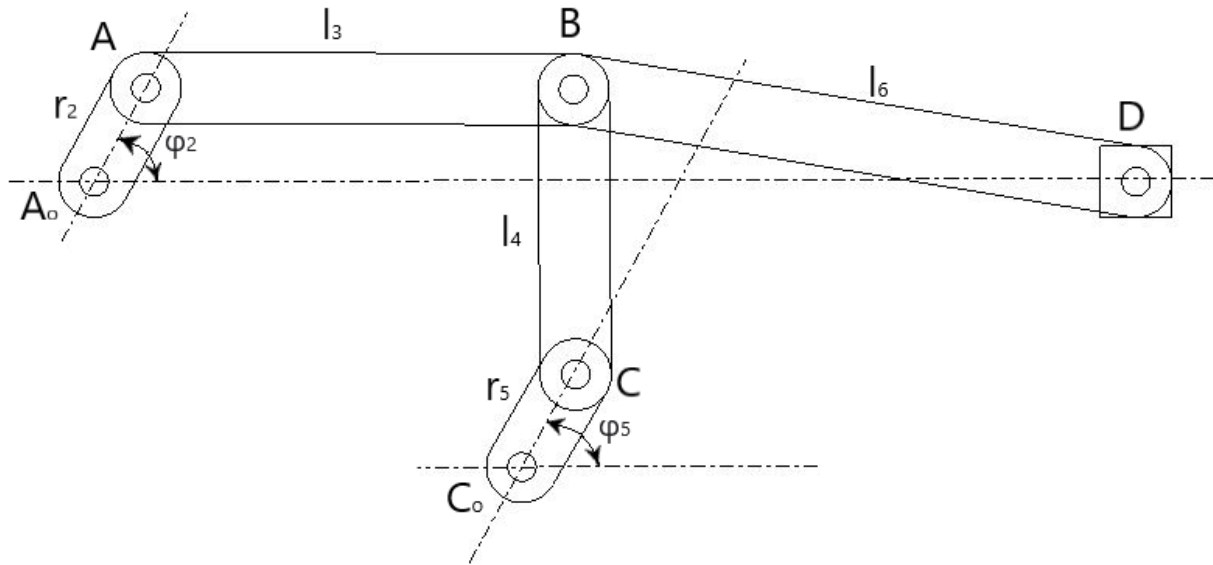


Figure 3.1: Line model of seven-bar mechanism

Where,

r_2 = radius of first eccentric (A_0A)

l_3 = length of link AB

l_4 = length of link BC

r_5 = radius of second eccentric (C_0C)

l_6 = length of link BD

φ_2 = first eccentric angle with respect to ground

φ_5 = second eccentric angle with respect to ground

3.2 Building of mechanism

First, schematic diagram of the design version done. A logical approach based on the assignment used to calculate dimensions of mechanism. For which coordinates of each point found with respect to origin considered A_0 . Length of link BD (l_6) found after calculating coordinate of point B, since following inequation should be satisfied in order to give proper slider mobility.

Equation 3.1: Condition to satisfy slider mobility

$$l_6 > B_x$$

Where,

B_x = coordinate of point B in x direction

The below range of values considered as recommendation for building of mechanism. Suitable values calculated using trial and error approach and further optimisation done to get accurate results.

3.2.1 Recommendation of length of links

3.2.1.1 Length of first eccentric r_2

Length of first eccentric r_2 , can be taken as half of required stroke length. The stroke requirement is in the range of 10-20 mm. Therefore, the recommended value for first eccentric r_2 can be in the range 5-10 mm.

3.2.1.2 Length of link l_3

Length of link l_3 taken from the general rule that length of connecting rod can be approximately three times the length of crank or eccentric. Therefore, the recommended value for link l_3 can be in the range 15-30 mm.

3.2.1.3 Length of link l_4

Length of link l_4 taken from the general rule that length of connecting rod can be approximately three times the length of crank or eccentric. Therefore, the recommended value for link l_3 can be in the range 15-30 mm.

3.2.1.4 Length of second eccentric r_5

Length of second eccentric r_5 taken from the required stroke length and from the difference between the maximum and minimum stroke.

3.2.1.5 Length of link l_6

In order to get the length of BD (l_6), we need to calculate coordinate of point B in x direction at that instant for the given initial angle set for both the eccentric A_oA (r_2) and C_oC (r_5). From the following picture shows a triangle, coordinate of point B in x direction found using below equation.

3.2.2 Equations of mechanism

This chapter describes the equations for calculating the coordinates of different points in the mechanism.

Equation 3.2: Equation to calculate coordinate of point B in x direction

$$B_x = A_x + l_3 \cos \delta$$

Where A_x is coordinate of point A in x direction and δ is angle from following picture.

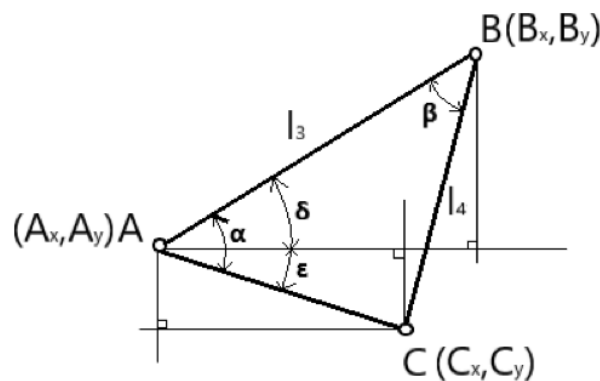


Figure 3.2: Triangle formed by points A, B, C

To calculate angle δ

Angle δ found using following equations.

Equation 3.3: Equation to calculate δ

$$\delta = \alpha - \varepsilon$$

Equation 3.4: Equation to calculate AC

$$AC = \sqrt{(A_y - C_y)^2 + (C_x - A_x)^2}$$

Equation 3.5: Equation to calculate α

$$\alpha = \cos^{-1} \left(\frac{l_3^2 + AC^2 - l_4^2}{2 * l_3 * AC} \right) \quad (\text{Using cosine theorem})$$

Equation 3.6: Equation to calculate ε

$$\varepsilon = \tan^{-1} \left(\frac{A_y - C_y}{C_x - A_x} \right)$$

To calculate A_x and A_y

Coordinates of point A in x direction (A_x) and y direction (A_y) found using following picture and equations.

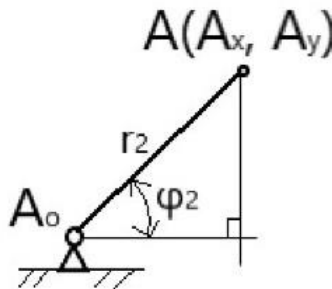


Figure 3.3: Triangle formed by Eccentric A_oA

Equation 3.7: Equation to calculate coordinate of point A in x direction

$$A_x = r_2 * \cos \varphi_2$$

Equation 3.8: Equation to calculate coordinate of point A in y direction

$$A_y = r_2 * \sin \varphi_2$$

To calculate C_x and C_y

Coordinates of point C in x direction (C_x) and y direction (C_y) found using following picture and equations.

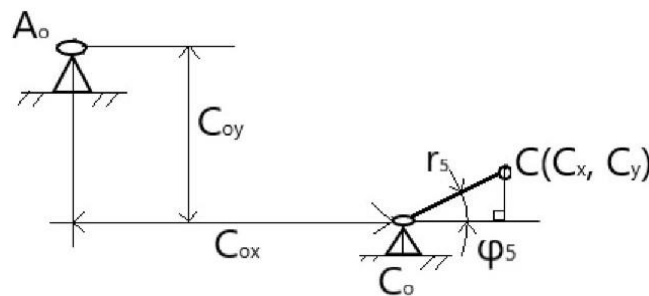


Figure 3.4 Triangle formed by Eccentric C_oC

Equation 3.9: Equation to calculate coordinate of point C in x direction

$$C_x = C_{ox} + r_5 * \cos \varphi_5$$

Equation 3.10: Equation to calculate coordinate of point C in y direction

$$C_y = -C_{oy} + r_5 * \sin \varphi_5$$

From the above equations, we got value of Bx using following expression.

Equation 3.11: Equation to calculate coordinate of point B in x direction

$$B_x = A_x + l_3 * \cos \delta$$

After getting the value of Bx, length of BD (l_6) can be found easily. The above values for the length of each links chosen will be analysed and optimised further for getting better results.

3.3 Selection of ground for second Eccentric

The position of C_o will be determined from difference between minimum and maximum stroke when the cranks were placed at both death centres. Point C_o placed at mean position of deviation of point B. The following pictures describes the change in stroke according to the death centres.

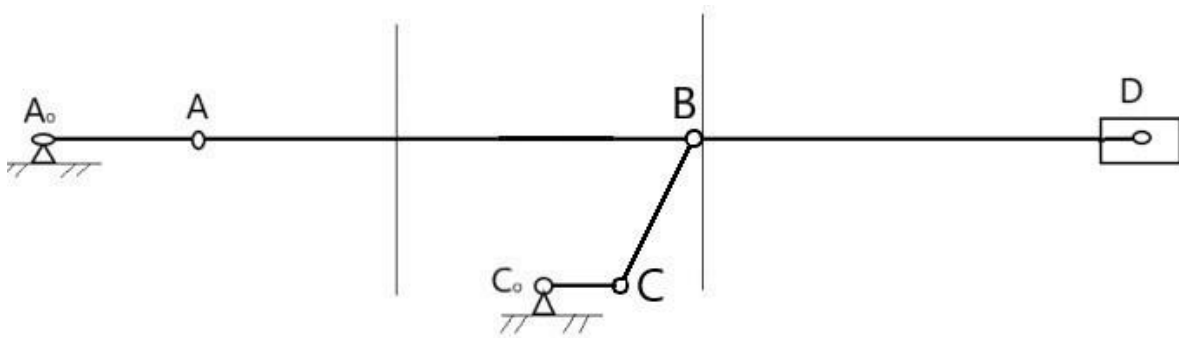


Figure 3.5: Selection of ground from first dead centre

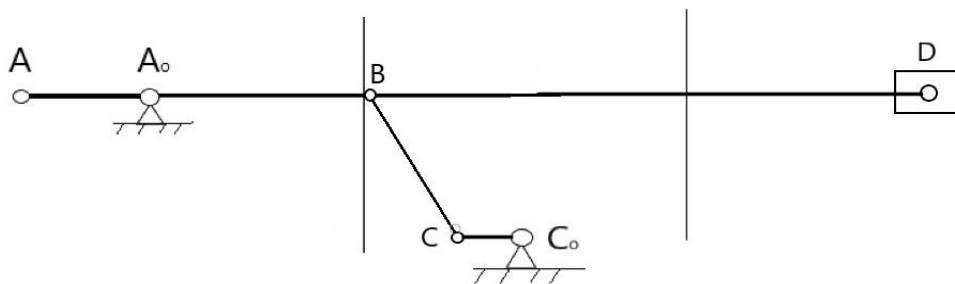


Figure 3.6: Selection of ground from second dead centre

4 DESIGN PROPOSAL

The research work done carried out initially with the help of patents. From the study and analysis of patent mechanism, length of links chosen randomly. Two different variants considered for this task and the best one chosen according to the slider stroke variation. The chosen variant built in PTC creo parametric and analysed as follows.

4.1 Requirement of mechanism

Requirement of the mechanism was to achieve the differential mechanism, which means we could get different slider travel distance by modifying eccentric angles (either φ_2 or φ_5). This solves the problem of getting varying slider travel distance without modifying mechanism physically i.e., no parts were modified or interchanged to get different slider travel distance. The range of slider travel distance required was between 10mm – 20mm. Upon multiple analysis between two versions, below results generated.

4.2 Variant-1

The proposal includes two variants. This chapter describes about variant-1. Variant-1 based on nine-bar mechanism in which there will be two sliders for the operation. The following diagram shows the line model of variant-1.

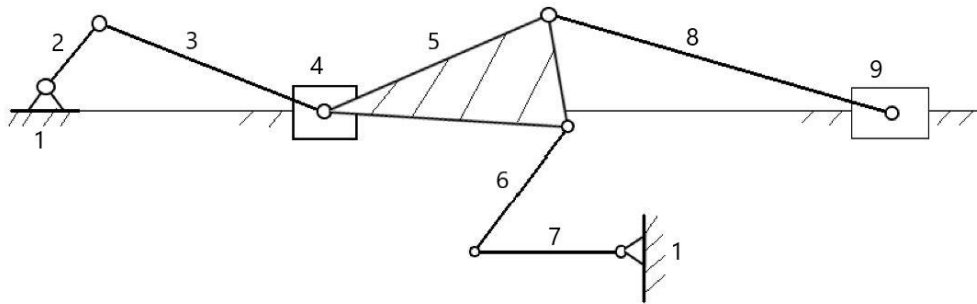


Figure 4.1: Line diagram for the variant-1

4.3 Variant-2

This chapter describes about variant-2. The proposal of variant-2 based on seven-bar mechanism, unlike the previous one, this proposal has one slider for the operation. The following diagram shows the line model of variant-2.

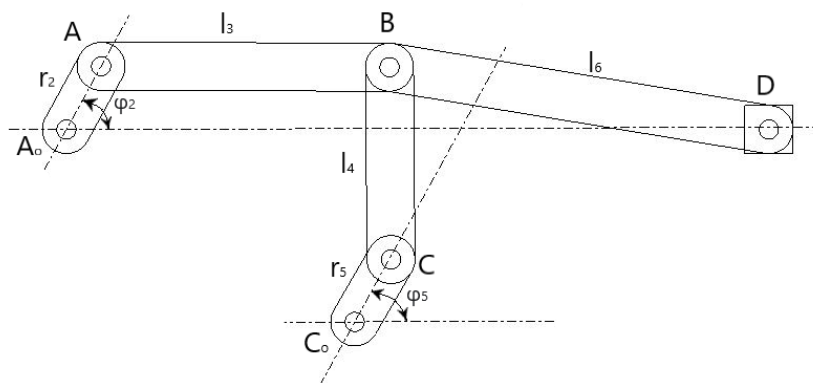


Figure 4.2: Line diagram for the variant-2

5 PROPOSED VARIANT

Variation-2 selected and processed further based on the simplicity and better mechanism building. The kinematic chain of seven-bar mechanism has comparatively less member than that of nine-bar mechanism. Since it has less number of members, it can have good functioning and cost of building reduced. This variant subdivided into two versions and the better one selected for the building of real model. The following describes about both the versions.

5.1 Version-1

The version-1 inspired from patent mechanism, modified as per our requirement and after multiple analysis below, values chosen for building the mechanism. The dimensions considered for the building of mechanism for version-1 are as following.

Distance of pivot C_o in x direction from pivot A_o (C_{ox}) = 30 mm.

Distance of pivot C_o in y direction from pivot A_o (C_{oy}) = 20 mm.

5.1.1 Initial structure

Initially the mechanism decided to build such that both eccentric placed in dead centre positions. Other links also followed such that all links fall along the axis of eccentric and link (BC) connecting both eccentric positioned perpendicular to eccentric axis. Initial structure designed according to transmission angle condition, which says transmission angle formed should be around 90° in optimum case. By arranging all links as per following picture, transmission angle formed will be 90° . The following picture shows the initial structure designed for the proposal.

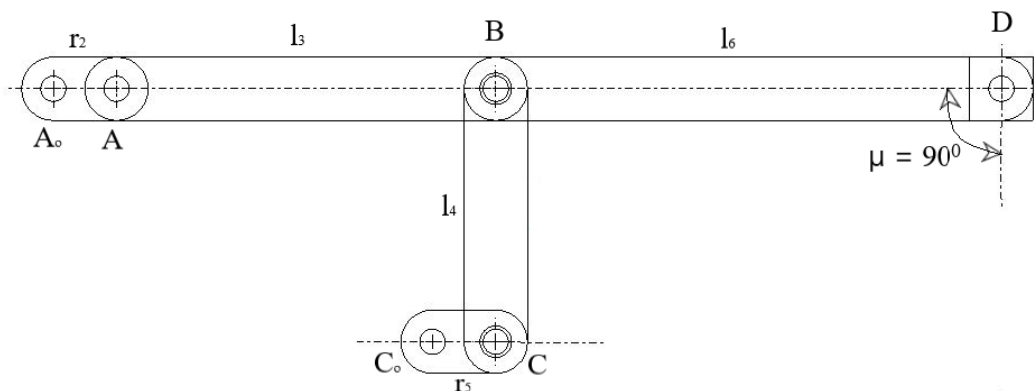


Figure 5.1: Line model of initial structure

5.1.1.1 Dimension of eccentric A_oA and C_oC

The dimensions of both eccentric A_oA (r_2) and C_oC (r_5) assumed to be equal in lengths. Since the required stroke length varies from 10 mm – 20 mm, the lengths of eccentric assumed as 5 mm – 10 mm each, initially which will be half of stroke length required and positioned in straight line as per figure 4.1.

5.1.1.2 Dimension of link AB

Length of link AB (l_3) chosen should satisfy the transmission angle condition which says the angle formed should be around 90° in optimum case. It can have deviation of around 40° to 50° during mechanism in operation. Considering the above conditions, multiple analysis done and dimension have been decided. From the analysis, the length of link AB (l_3) taken as 30 mm and positioned along axis of eccentric A_oA as per figure 4.1.

5.1.1.3 Dimension of link BC

When the link AB positioned along axis of eccentric A_0A in straight line, the perpendicular distance from point B to point C from above figure 4.1 comes out to be around 20 mm. This dimension chosen as the length of link BC (l_4) and positioned as per figure 4.1.

5.1.1.4 Dimension of link BD

Length of link BD (l_6) chosen such that following equation should be satisfied in order to give proper slider mobility.

Equation 5.1: Equation to satisfy slider mobility

$$l_6 > B_x$$

Where, B_x = coordinate of point B in x direction. From the above equation, B_x comes out to be around 35 mm. Therefore, the length of link BD taken as 40 mm, which also satisfied transmission angle condition and positioned in straight line as per figure 4.1.

5.1.2 Analysis of stroke variation for initial structure

When the mechanism of initial structure put to operation, slider travel can be analysed. The following dimensions of both eccentric considered for the analysis.

5.1.2.1 Stroke variation 10 mm

The length of both eccentric taken as 5 mm and the analysis carried out. The following picture shows the eccentric angle ϕ_2 and ϕ_5 between them.

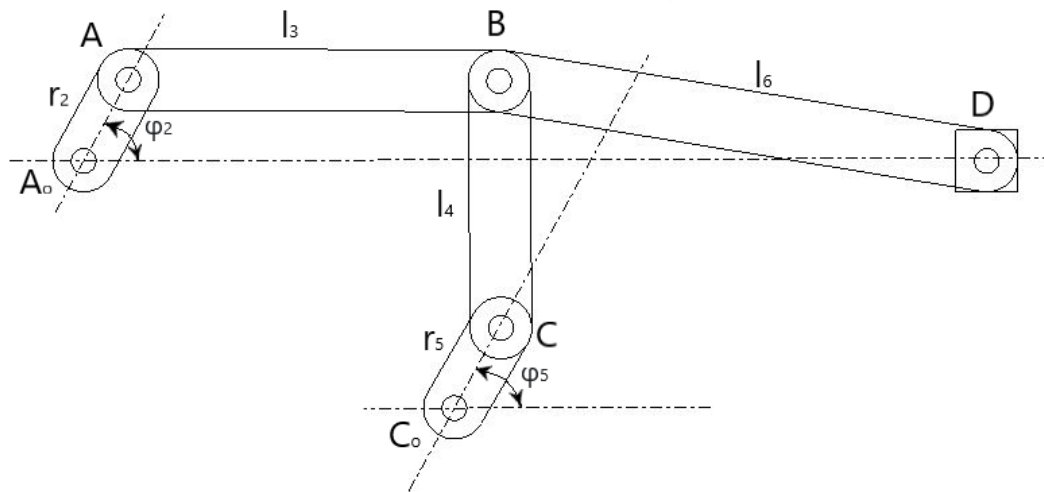


Figure 5.2: Line model showing eccentric angles

Phase difference between both the eccentric ($\phi_2 - \phi_5$) varied from $0^\circ - 360^\circ$ in order to get the stroke variation for different phase difference between them. The following picture shows the stroke variation for different phase difference between both the eccentric when the length of both eccentric taken as 5 mm.

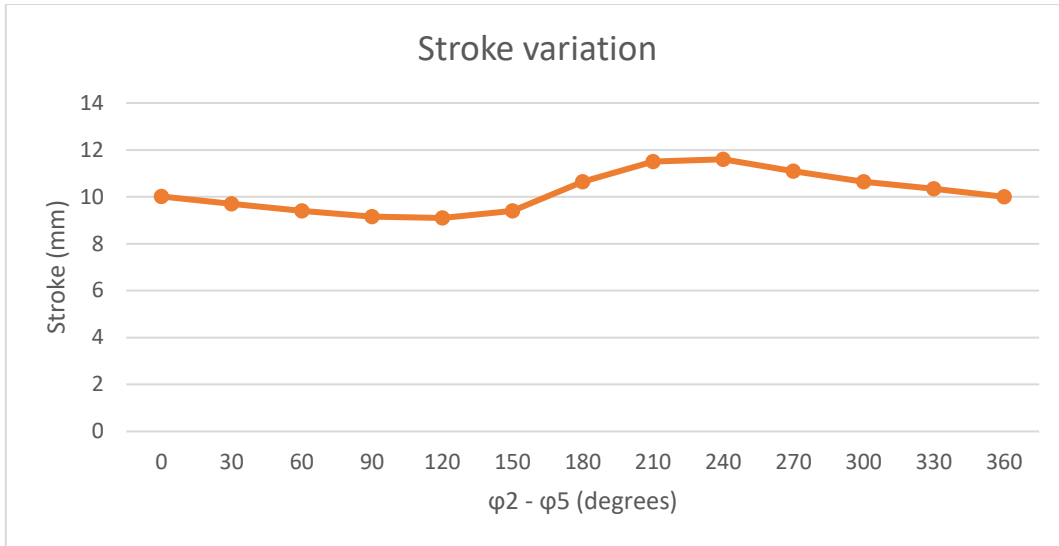


Figure 5.3: Stroke variation when length of both eccentrics are 5 mm

5.1.2.2 Stroke variation 20 mm

The dimensions of all the links doubled and the analysis carried out. Phase difference between both the eccentric ($\phi_2 - \phi_5$) varied from $0^\circ - 360^\circ$ in order get the stroke variation for different phase difference between both the eccentrics. For this stroke variation of 20 mm achieved, the dimensions modified and the transmission angle conditions satisfied. The following picture shows the stroke variation for different phase difference between both the eccentrics when the length of both eccentrics taken as 10 mm.

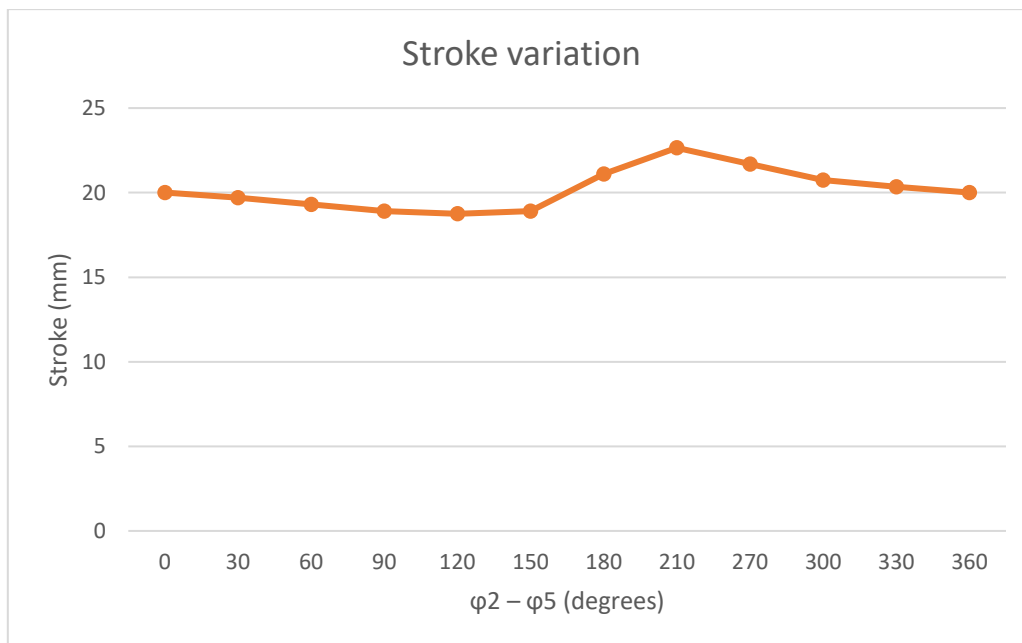


Figure 5.4: Stroke variation when length of both eccentrics are 10 mm

The following table shows the comparison of stroke variation for different eccentric lengths.

Table 5.1: Comparison of stroke variation for different eccentric lengths

Eccentric length	Maximum stroke	Minimum stroke
5 mm	11.5 mm	9 mm
10 mm	22.5 mm	18.5 mm

From the above table and picture representing stroke variation for respective eccentric lengths, it is clear that there is very less range of stroke variation. Therefore, the modification of mechanism has done to get desired stroke range.

5.1.3 Modified structure

The required stroke range should vary from 10 mm – 20 mm, so the modification of structure of the mechanism needed to achieve the desired stroke range. Many trials done in order to get the required stroke range. Modification of all the links in terms of change of dimensions done. Structure of mechanism changed by changing the positioning of link BC from previous version. Change of structure done considering the transmission angle condition. Modified structure has the transmission angle around 75° , which is good for functioning of mechanism. The following picture shows modified structure by changing positioning of link BC and modifying dimensions of all the links.

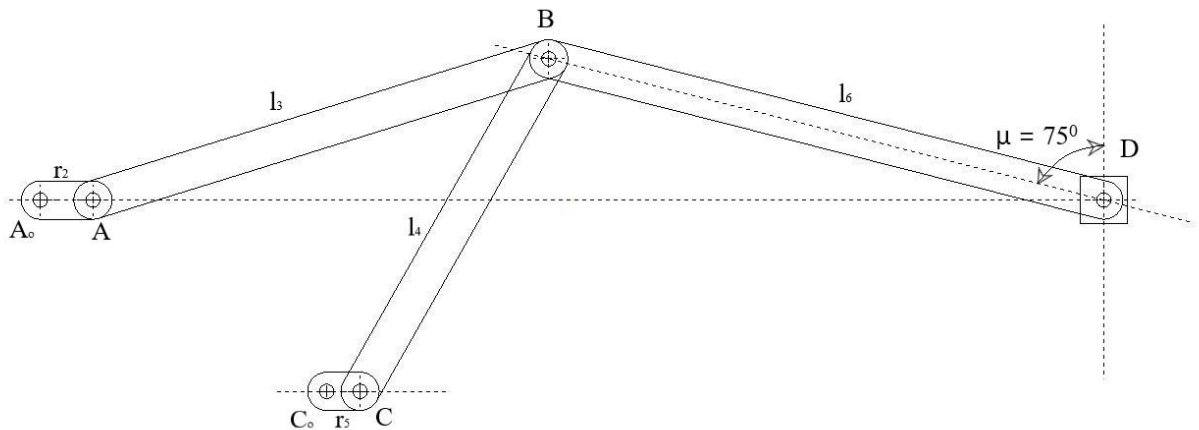


Figure 5.5: Line model of modified structure

5.1.3.1 Dimension of link AB

Length of link AB (l_3) chosen should satisfy the transmission angle condition which says the angle formed should be around 90° in optimum case. It can have deviation of around 40° to 50° during mechanism in operation. Considering the above conditions, multiple analysis done and dimension have been decided. From the analysis, the length of link AB (l_3) taken as 50 mm and transmission angle of around 75° formed which also satisfies its condition.

5.1.3.2 Dimension of link BC

Position of link BC (l_4) modified from its previous version so that the range of stroke variation will be more. Length of BC chosen should also satisfy the transmission angle condition. From multiple values and respective analysis, the length of link BC taken as 40 mm, which also satisfies transmission angle condition.

5.1.3.3 Dimension of link BD

Length of link BD (l_6) chosen such that following equation should be satisfied in order to give proper slider mobility.

Equation 5.2: Equation to satisfy slider mobility

$$l_6 > B_x$$

Where, B_x = coordinate of point B in x direction. From the above equation, B_x comes out to be around 53 mm. Therefore, the length of link BD taken as 60 mm, which also satisfied transmission angle condition.

5.1.3.4 Dimension of eccentrics A_oA and C_oC

The dimensions of both eccentrics A_oA (r_2) and C_oC (r_5) varied from their previous versions. Many trials done for selecting the dimensions such that the stroke range comes within 10 mm – 20 mm. A range of values chosen and respective analysis done. For each combination of eccentric lengths of A_oA and C_oC , motion analysis done and stroke length found. Phase difference between both the eccentrics varied from $0^\circ - 360^\circ$ and motion analysis done. This analysis clearly shows changing phase difference between both, the eccentric results in different stroke length. The stroke variation achieved also tried to adjust between 10 mm – 20 mm. The following picture shows the analysis done for different combination of eccentric lengths and its respective stroke variation for different phase difference between both the eccentrics.



Figure 5.6: Stroke variation for different combination of eccentric lengths

From the above picture, it is clear that combination of 5.5 mm and 3.5 mm eccentric lengths for A_oA and C_oC respectively is good and gives stroke range of 10 mm – 20 mm. The following picture shows the stroke variation for the chosen combination of eccentric lengths for different phase difference between both the eccentrics.

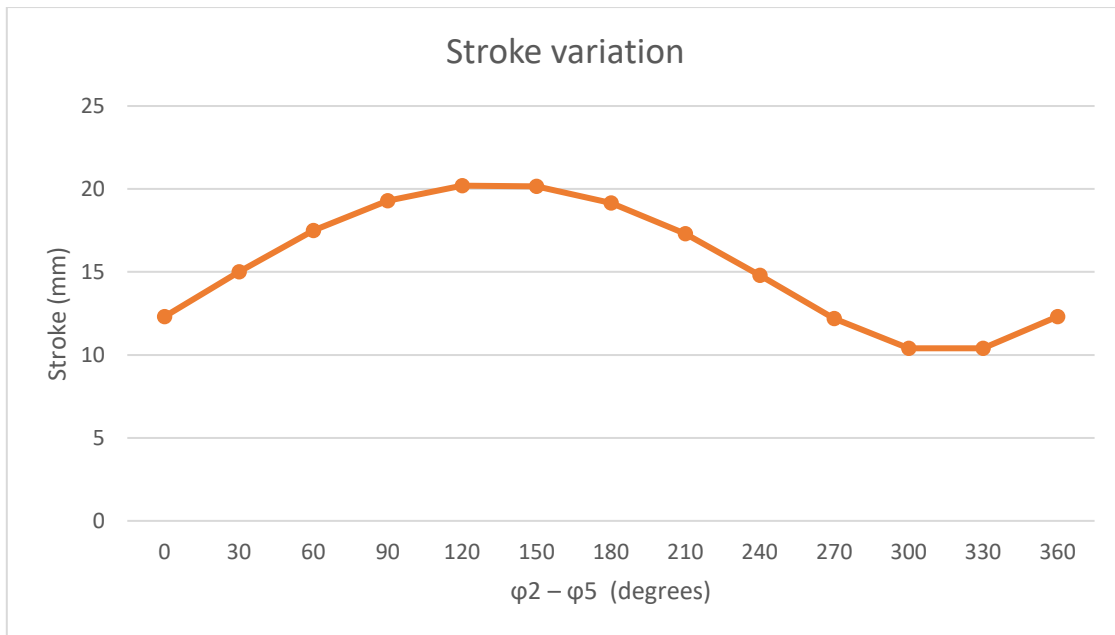


Figure 5.7: Stroke variation for selected eccentric lengths

The following table shows the details of stroke for each difference in eccentric angle between them.

Table 5.2: Stroke variation for selected eccentric lengths

Phase difference (degrees)	Stroke (mm)
0 ⁰	12
30 ⁰	15
60 ⁰	17.5
90 ⁰	19
120 ⁰	20
150 ⁰	20
180 ⁰	19
210 ⁰	17
240 ⁰	15
270 ⁰	12
300 ⁰	10
330 ⁰	10.5
360 ⁰	12

5.1.4 Final structure of version-1

After the analysis of each links and finalising its dimensions, the line model of version-1 looks like the following picture.

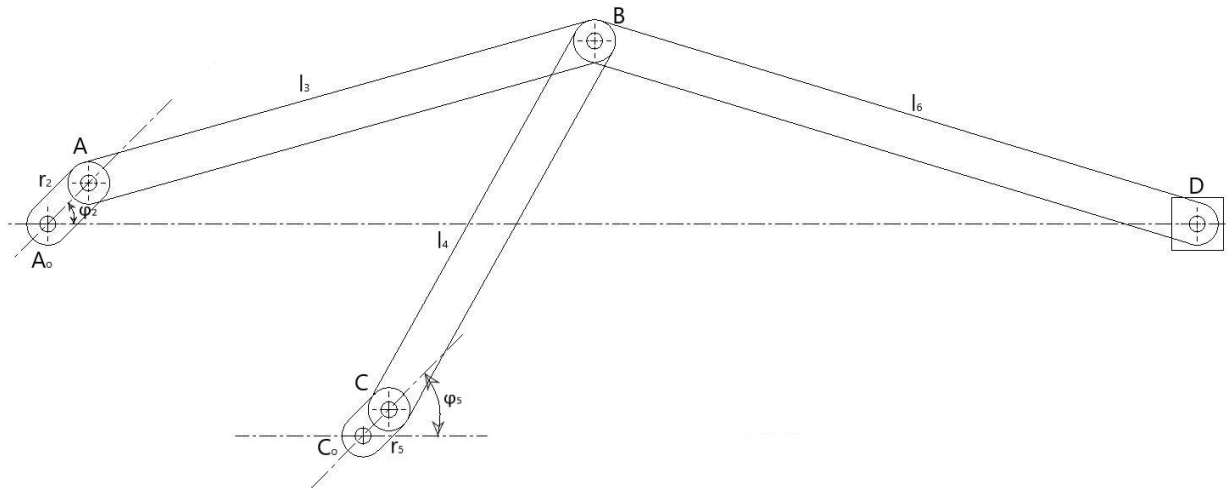


Figure 5.8: Final structure of version-1

5.1.5 Analysis of radial forces of version-1

The radial force acting at the joint A, B, C, D has to be analysed in process of bearing selection. According to the force acting at the particular joint, respective bearing chosen. The following are the analysis at the joints where bearings are required.

5.1.5.1 Radial force at joint A

Dynamic analysis performed and the radial force acting at their joint found. Following chart shows the variation of radial force at the joint A.

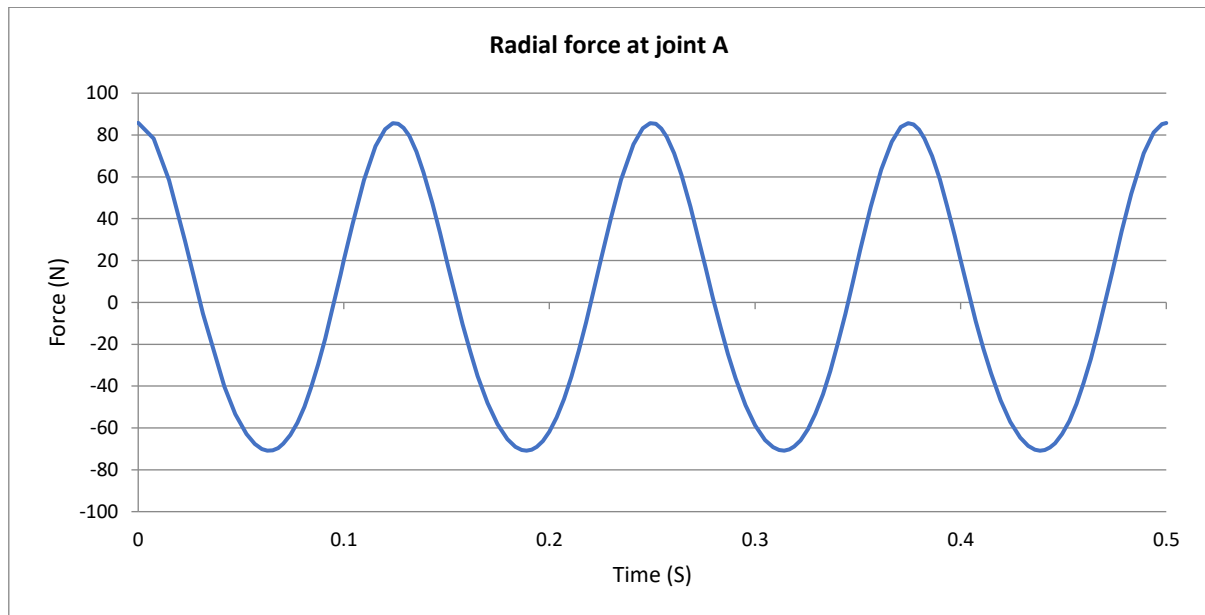


Figure 5.9: Radial force at joint A

5.1.5.2 Radial force at joint B

Dynamic analysis performed and the radial force acting at their joint found. Following chart shows the variation of radial force at the joint B.

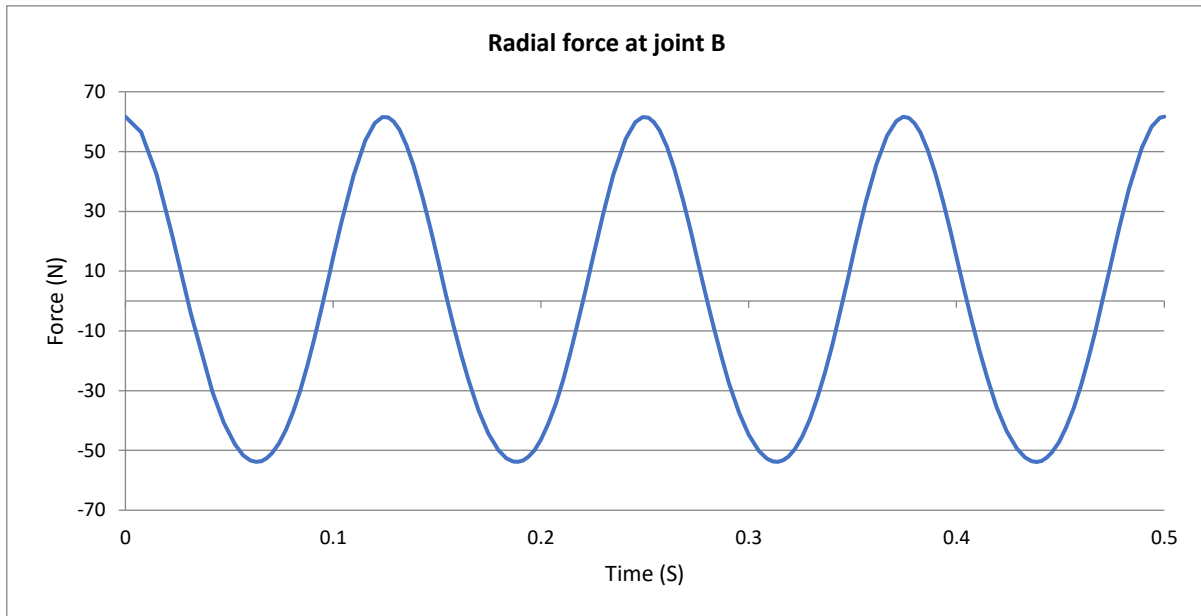


Figure 5.10: Radial force at joint B

5.1.5.3 Radial force at joint C

Dynamic analysis performed and the radial force acting at their joint found. Following chart shows the variation of radial force at the joint C.

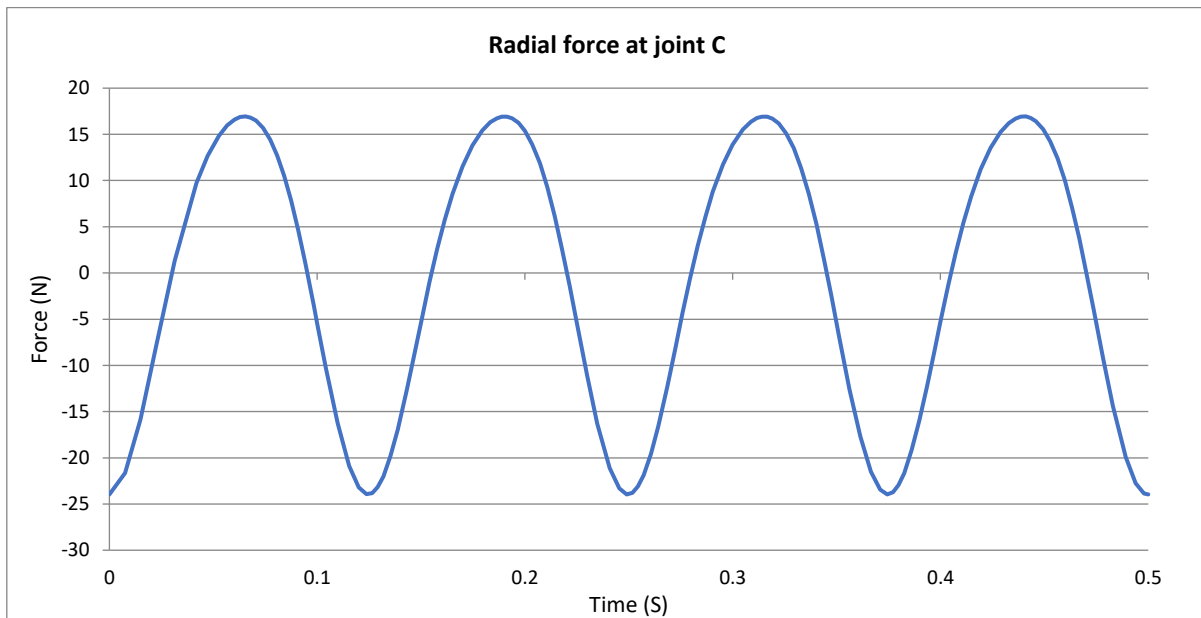


Figure 5.11: Radial force at joint C

5.1.6 Bearing selection

Following table shows the comparison of all radial forces acting across joints.

Table 5.3: Comparison of radial forces across joints

Joint	Maximum radial force (N)
A	85 N
B	60 N
C	18 N

From the above table it is clear that there is very less variation in their radial forces. Therefore, same bearing can be utilised across all the joints.

5.2 Version-2

Another new version done and analysis carried out. Resulting better proposal than previous one. Analysis of slider travel distance carried out and gave good match for the requirement. This version gave better harmonic sinusoidal wave of resulting slider analysis.

The following changes made for making this proposal better than previous one,

- Eccentric shafts have been used
- One of the binary link has been replaced by a ternary link

The following picture shows the line diagram of the version-2.

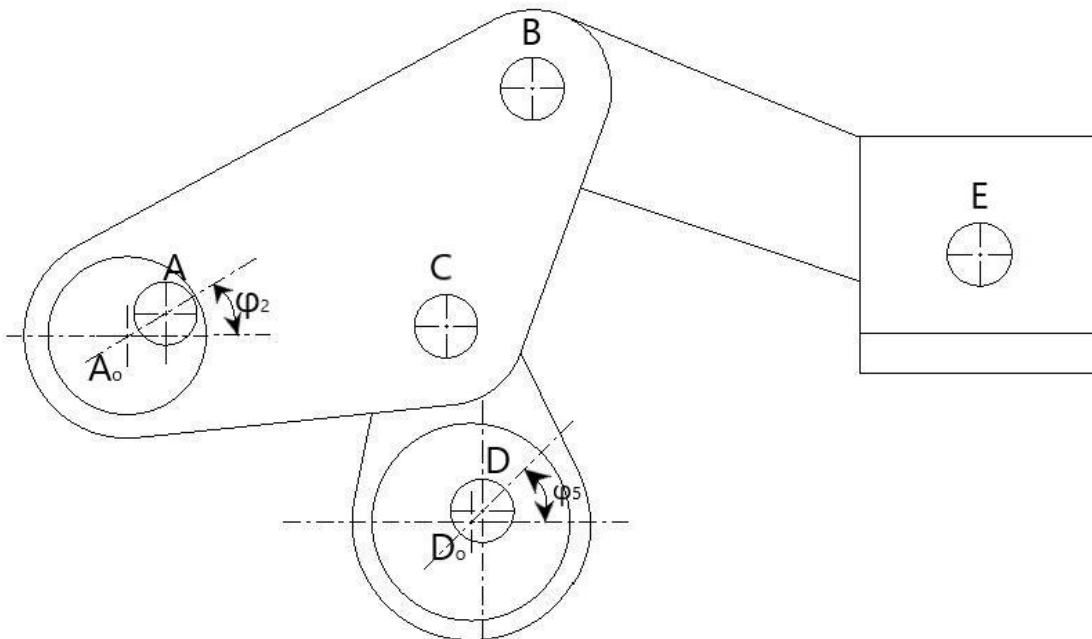


Figure 5.12: Line diagram of version-2

5.2.1 Building of mechanism

This version is updated version of previous one. The dimensions of this version mostly influenced from the previous version. From the above figure 5.12, coordinates of each point found with respect to origin considered as A_0 . The following equation should be satisfied in order to give proper slider mobility.

Equation 5.3: Equation to satisfy slider mobility

$$BE > B_x$$

Where,

B_x = coordinate of point B in x direction

The below range of values considered for building of mechanism. Suitable values calculated using trial and error approach and further optimisation done to get accurate results.

$$A_oA = 3-7 \text{ mm}$$

$$A_oB = 55-65 \text{ mm}$$

$$BC = 25-35 \text{ mm}$$

$$A_oC = 35-45 \text{ mm}$$

$$CD = 20-30 \text{ mm}$$

$$C_oC = 1-2 \text{ mm}$$

In order to get the length of BE, we need to calculate coordinate of point B in x direction at that instant for the given initial angle set for both the eccentric A_oA and D_oD . From the following picture shows a triangle, coordinate of point B in x direction found using following equation.

Equation 5.4: Equation to calculate coordinate of point B in x direction

$$B_x = A_x + l_3 \cos \delta$$

Where A_x is coordinate of point A in x direction and δ is angle from following picture.

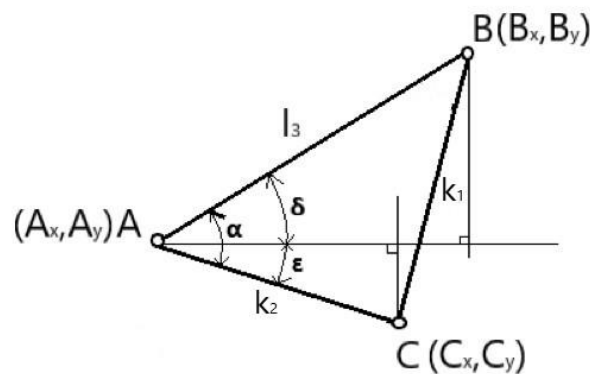


Figure 5.13: Triangle formed by points A, B, C

To calculate angle δ

Angle δ found using following equations

Equation 5.5: Equation to calculate δ

$$\delta = \alpha - \epsilon$$

Equation 5.6: Equation to calculate α

$$\alpha = \cos^{-1} \left(\frac{l_3^2 + k_2^2 - k_1^2}{2 * l_3 * k_2} \right) \quad (\text{Using cosine theorem})$$

Equation 5.7: Equation to calculate ε

$$\varepsilon = \tan^{-1} \left(\frac{A_y - C_y}{C_x - A_x} \right)$$

To calculate A_x and A_y

Coordinates of point A in x direction (A_x) and y direction (A_y) found using following picture and equations.

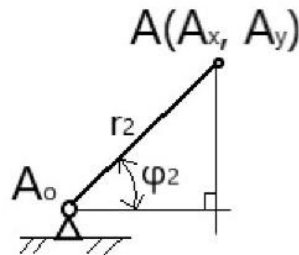


Figure 5.14: Triangle formed by eccentric A_oA

Equation 5.8: Equation to calculate coordinate of point A in x direction

$$A_x = r_2 * \cos \varphi_2$$

Equation 5.9: Equation to calculate coordinate of point A in y direction

$$A_y = r_2 * \sin \varphi_2$$

To calculate C_x and C_y

Coordinates of point C in x direction (C_x) and y direction (C_y) found using following picture and equations.

Equation 5.10: Equation to calculate coordinate of point C in x direction

$$C_x = A_x + k_2 \cos \delta$$

Equation 5.11: Equation to calculate coordinate of point C in y direction

$$C_y = A_y + k_2 \sin \delta$$

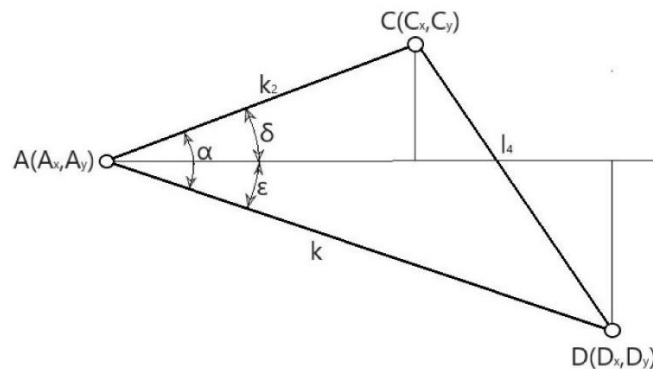


Figure 5.15: Triangle formed by points A, C, D

To calculate angle δ

Angle δ found using following equations

Equation 5.12: Equation to calculate δ

$$\delta = \alpha - \varepsilon$$

Equation 5.13: Equation to calculate α

$$\alpha = \cos^{-1} \left(\frac{k_2^2 + k^2 - l_4^2}{2 * k * k_2} \right) \quad (\text{Using cosine theorem})$$

Equation 5.14: Equation to calculate ε

$$\varepsilon = \tan^{-1} \left(\frac{A_y - D_y}{D_x - A_x} \right)$$

To calculate D_x and D_y

Coordinates of point D in x direction (D_x) and y direction (D_y) found using following picture and equations.

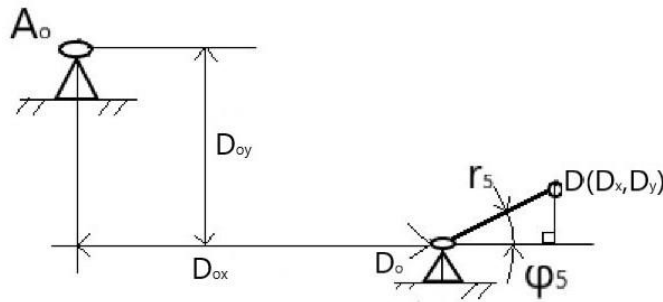


Figure 5.16: Triangle formed by eccentric D_0D

Equation 5.15: Equation to calculate point D in x direction

$$D_x = D_{0x} + r_5 * \cos \varphi_5$$

Equation 5.16: Equation to calculate point D in y direction

$$D_y = -D_{0y} + r_5 * \sin \varphi_5$$

From the above equations, we got value of B_x using following expression

Equation 5.17: Equation to calculate point B in x direction

$$B_x = A_x + l_3 * \cos \delta$$

After getting the value of B_x , length of BE (l_6) can be found easily. The above values for the length of each links chosen will be analysed and optimised further for getting better results.

5.2.2 Dimension of eccentrics

Initially eccentric radius and lengths of other links chosen as a range of values and did analysis on the same to get suitable results. In this version, eccentric used and one of the binary link replaced with a ternary link unlike previous version. Their values have discussed as follows,

Eccentric of shaft 1 = 3 - 7 mm.

Eccentric of shaft 2 = 1 - 2 mm.

The eccentric's value for each eccentric chosen such that the slider travel should have stroke range of 10 - 20 mm. Many trials done before getting the suitable value for eccentrics. The dimension of other links chosen to match the stroke range of 10 - 20 mm.

The following picture shows the stroke variation for each eccentrics for different phase difference between both the eccentrics.

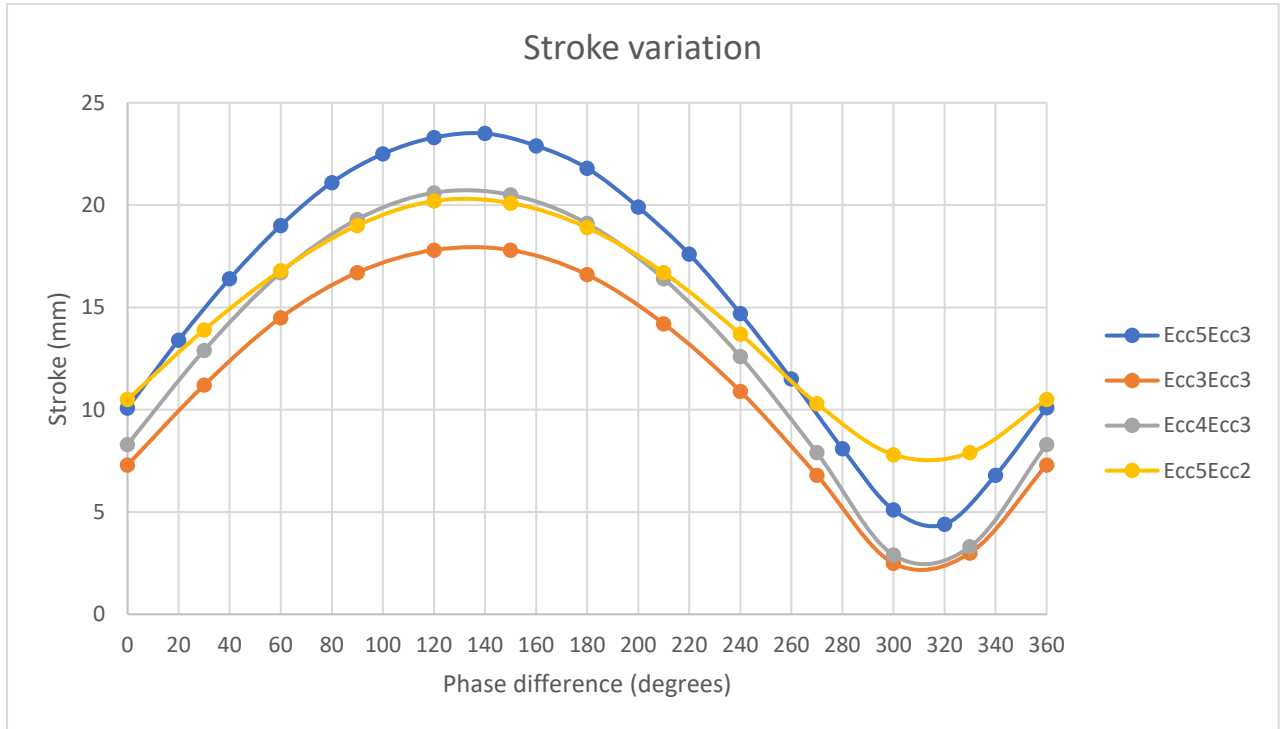


Figure 5.17: Stroke variation for different values of eccentrics

The following table shows the maximum and minimum stroke achieved from the different values of eccentrics.

Table 5.4: Stroke variation for different values of eccentrics

Eccentrics 1 (mm)	Eccentrics 2 (mm)	Maximum stroke (mm)	Minimum stroke (mm)
5 mm	3 mm	23.5 mm	4.5 mm
3 mm	3 mm	18 mm	2.5 mm
4 mm	3 mm	20.5 mm	3 mm
5 mm	2 mm	20 mm	8 mm

After multiple trials, for each eccentric values we got suitable range of stroke around 10 - 20 mm. The values of the eccentrics of each eccentric from which stroke range of 10 - 20 mm achieved are as follows,

Eccentric 1 = 5.6 mm

Eccentric 2 = 2 mm

The following graph shows the variation of stroke for each difference in eccentric angle between them.

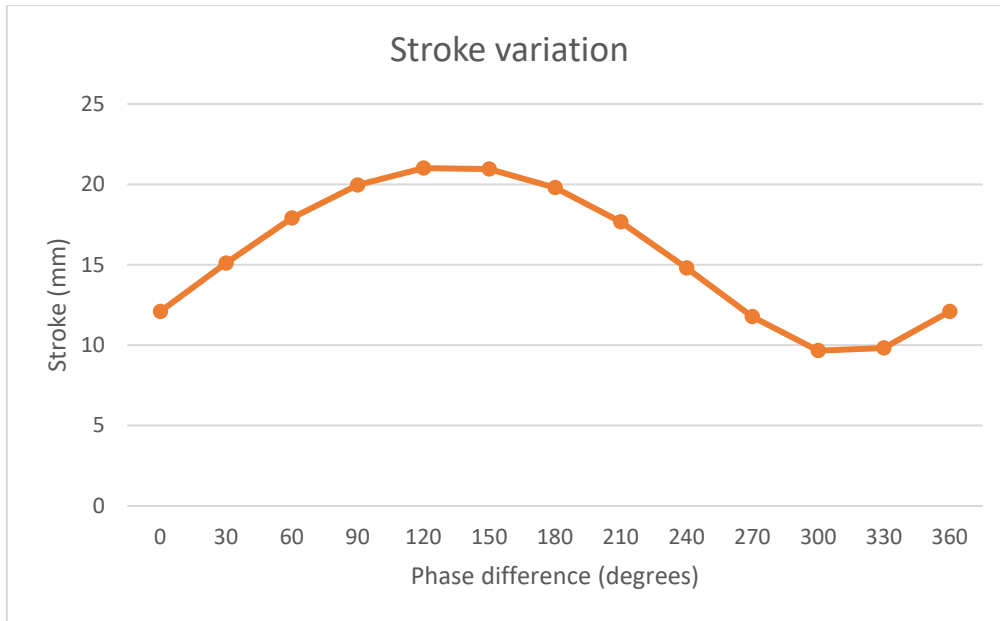


Figure 5.18: Stroke variation for chosen eccentrics

From the above graph, it is clear that the chosen eccentric is suitable to get the stroke range of 10 - 20 mm. The below table shows the details of stroke for each difference in eccentric angle between them.

Table 5.5: Stroke variation for chosen eccentrics

Phase difference (degrees)	Stroke (mm)
0 ⁰	12
30 ⁰	15
60 ⁰	18
90 ⁰	20
120 ⁰	21
150 ⁰	21
180 ⁰	20
210 ⁰	17.5
240 ⁰	15
270 ⁰	12
300 ⁰	9.5
330 ⁰	10
360 ⁰	12

5.2.3 Optimization of slider axis

After determining proper eccentric's values, the stroke range came very close to the required range of 10 - 20 mm but still not fully matching. In order to make it fully match, the value of e is modified, which is the displacement of axis of slider to the axis of eccentrics one. The following picture shows the displacement of slider axis to the eccentric one axis.

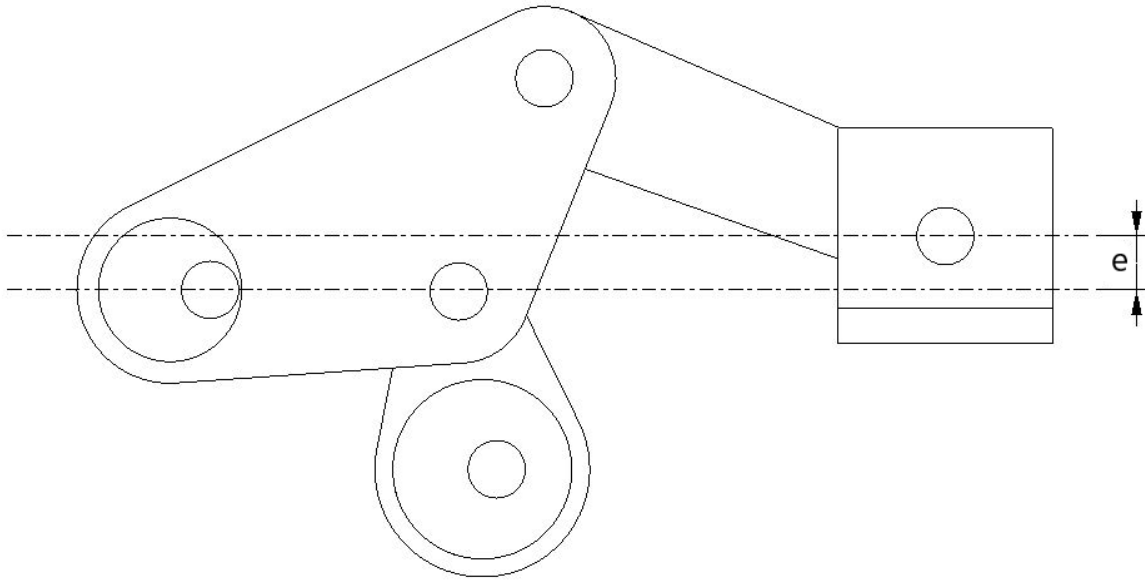


Figure 5.19: Displacement of slider axis to the eccentric 1 axis

Without such displacement, the stroke variation is not in the range of 10 - 20 mm. The following shows the deviation when the mechanism was built with displacement and without displacement.

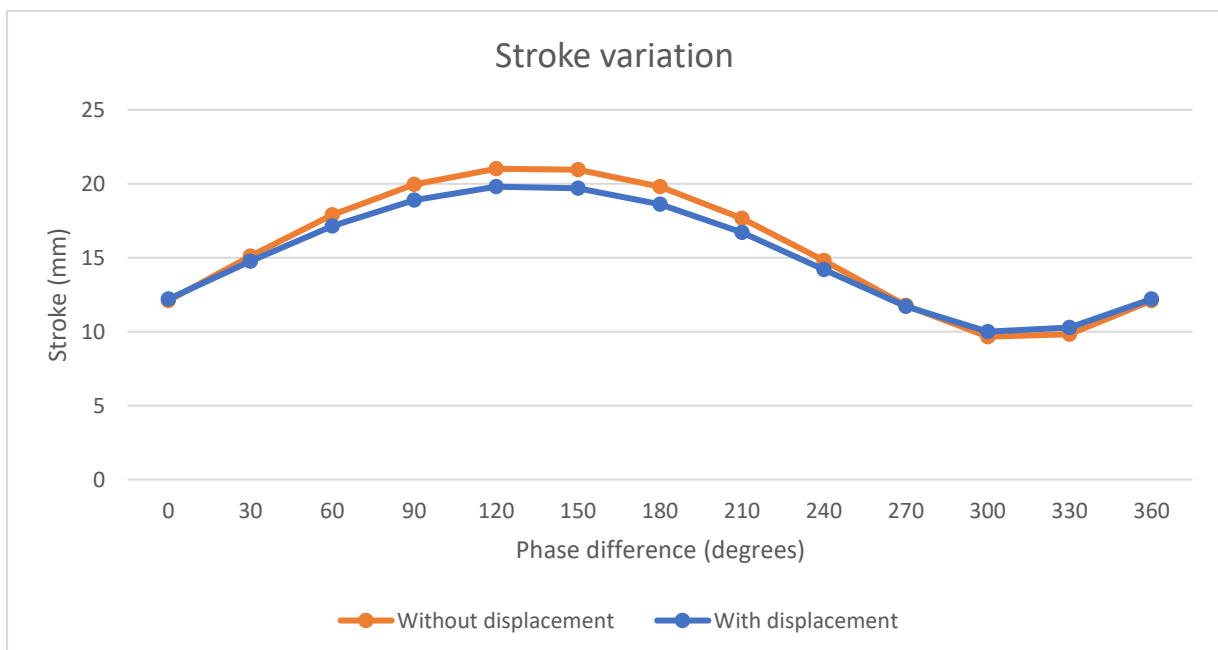


Figure 5.20: Stroke variation for slider axis displacement

From the above picture, it is clear that when the slider displaced by the value of e , there is good match of required stroke range of 10 - 20 mm. From multiple trials, the value of e found shown below,

$$e = 7.5 \text{ mm}$$

The following picture and table shows the details of stroke for each difference in eccentric angle between them when the slider displaced by the value of 7.5 mm.

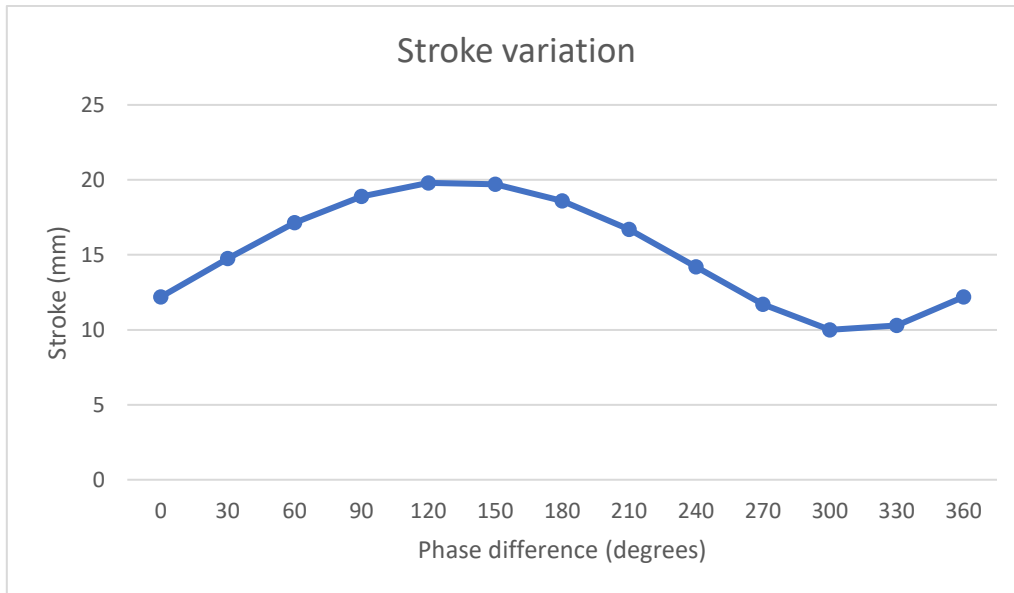


Figure 5.21: Stroke variation when slider displaced by 7.5 mm

Table 5.6: Stroke variation when slider displaced by 7.5 mm

Phase difference (degrees)	Stroke (mm)
0 ⁰	12
30 ⁰	15
60 ⁰	17
90 ⁰	19
120 ⁰	20
150 ⁰	20
180 ⁰	18.5
210 ⁰	16.5
240 ⁰	14
270 ⁰	11.5
300 ⁰	10
330 ⁰	10
360 ⁰	12

6 BUILDING OF REAL MODEL

The dimensions of all the parts found, the next step in the process is to use those and build into a real model. The following shows how each parts modified for building into the real model and assembly of those parts done.

6.1 Design of links

In this chapter, we see about how all the links modified to make it the real model as follows.

6.1.1 Eccentric shaft 1

The shaft made eccentric to match the condition. The eccentric shaft is made of E335 steel material. Initially the material taken from standard dimension in the form of circular rod, then machined using CNC machine as per the dimensions. The value of eccentric of shaft 1 shown below and the following picture shows the CAD model made for the eccentric shaft 1.

Eccentric 1 = 5.6 mm.



Figure 6.1: Eccentric shaft 1

6.1.2 Eccentric shaft 2

The shaft made eccentric to match the condition. The eccentric shaft is made of E335 steel material. Initially the material taken from standard dimension in the form of circular rod, then machined using CNC machine as per the dimensions. The value of eccentric of shaft 2 shown below and the following picture shows the CAD model made for the eccentric shaft 2.

Eccentric 2 = 2 mm.



Figure 6.2: Eccentric shaft 2

6.1.3 Ternary link

The ternary link modified to facilitate the building of real model. The ternary link is made of E335 steel material. Initially the material taken from standard dimension in the form of rectangular block, then machined using CNC machine as per dimensions. The following picture shows the CAD model made for the ternary link.

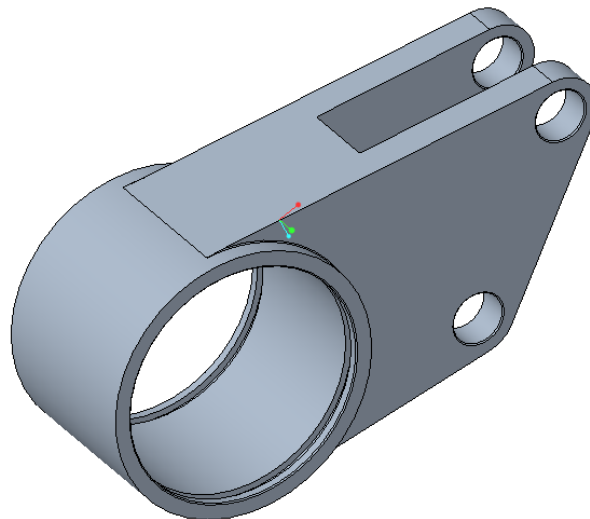


Figure 6.3: Ternary link

6.1.4 Connecting rod 1

The connecting rod 1 modified to facilitate the building of real model. The connecting rod is made of E335 steel material. Initially the material taken from standard dimension in the form of rectangular block, then machined using CNC machine as per dimensions. The following picture shows the CAD model made for the connecting rod 1.

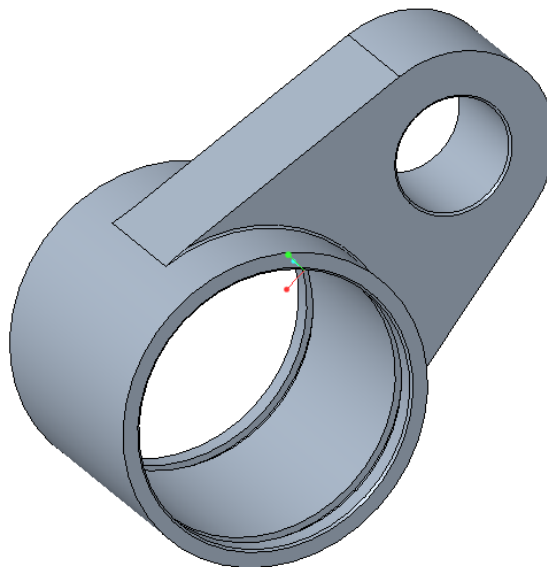


Figure 6.4: Connecting rod 1

6.1.5 Connecting rod 2

The connecting rod 2 modified to facilitate the building of real model. The connecting rod 2 is made of E335 steel material. Initially the material taken from standard dimension in the form of rectangular block, then machined using CNC machine as per dimensions. The following picture shows the CAD model made for the connecting rod 2.

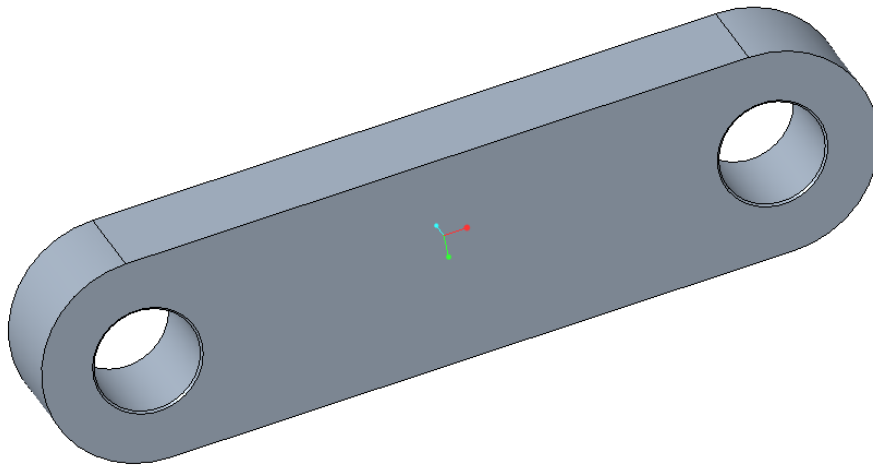


Figure 6.5: Connecting rod 2

6.1.6 Slider joint

The part connecting the slider to the connecting rod modified to facilitate the building of real model. The slider joint is made of E335 steel material. Initially the material taken from standard dimension in the form of rectangular block, then machined using CNC machine as per dimensions. The following picture shows the CAD model made for the slider joint.

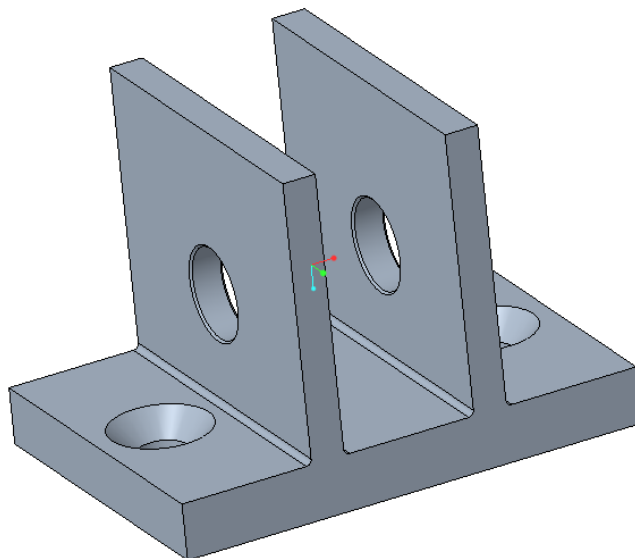


Figure 6.6: Slider joint

6.2 Selection of slider

The slider translates along X-axis direction to the mechanism. It carries the output from the mechanism to move in the horizontal linear motion. It carries the required stroke variation of 10 - 20 mm. Since a very small stroke, variation is required, the miniature linear guide chosen. The following picture shows the CAD model of the linear guide.

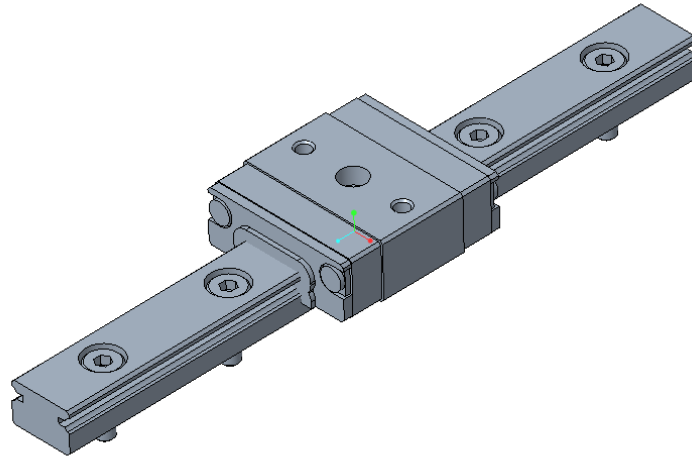


Figure 6.7: Linear guide

6.3 Selection of bearing

After selecting appropriate dimension of the links and eccentrics. The next step was to perform dynamic analysis of above mechanism at their revolute joints. This was necessary for the selection of appropriate bearings according to the exerted force. The following explains about how the force acting at each joint and selection of respective bearings.

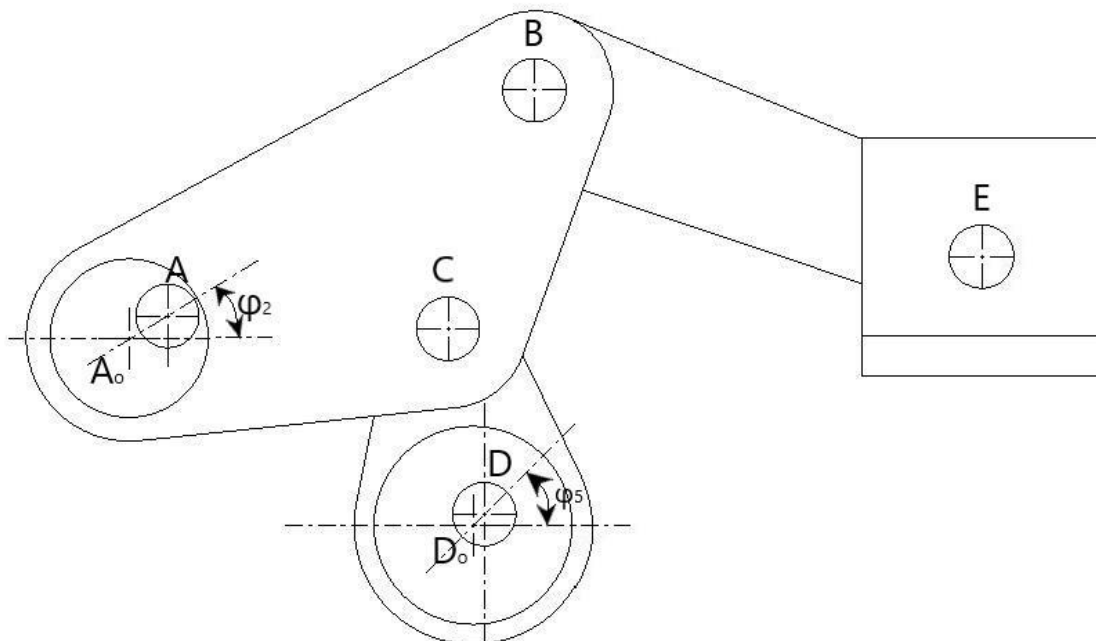


Figure 6.8: Line diagram of version-2

6.3.1 Radial force at eccentric 1 (A_0A) in x direction

Dynamic analysis performed and the radial force acting at their joint found. Following chart shows the variation of radial force at the eccentrics A_0A in x direction.

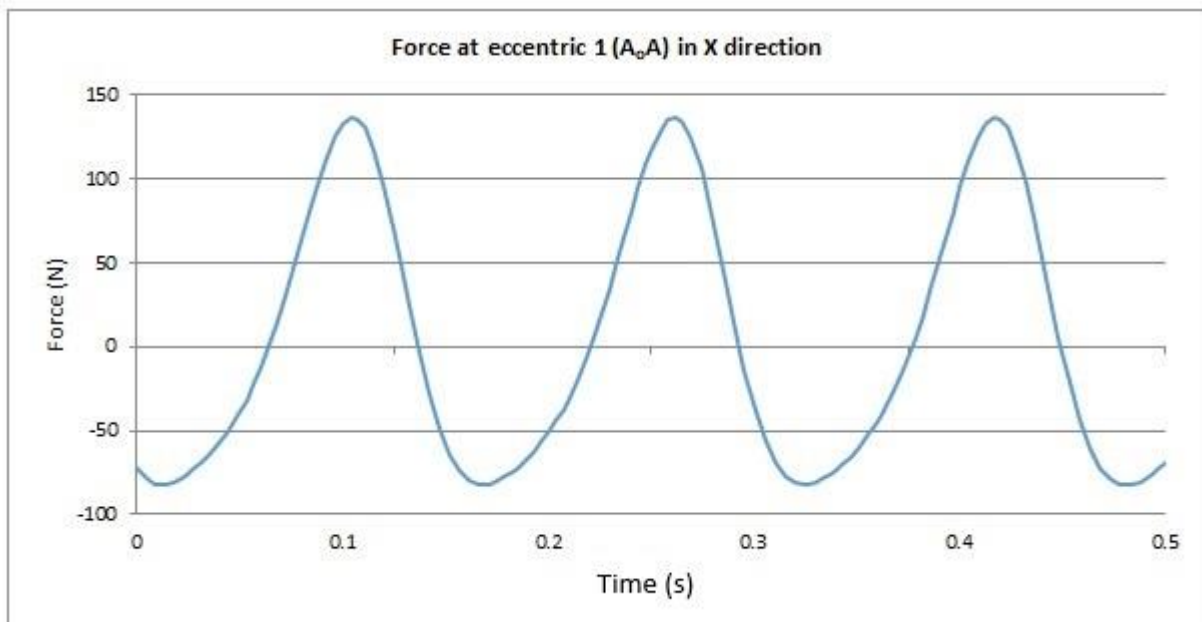


Figure 6.9: Radial force at eccentric1 (A_0A) in X direction

6.3.2 Radial force at eccentric 1 (A_0A) in y direction

Dynamic analysis performed and the radial force acting at their joint found. Following chart shows the variation of radial force at the eccentrics A_0A in y direction.

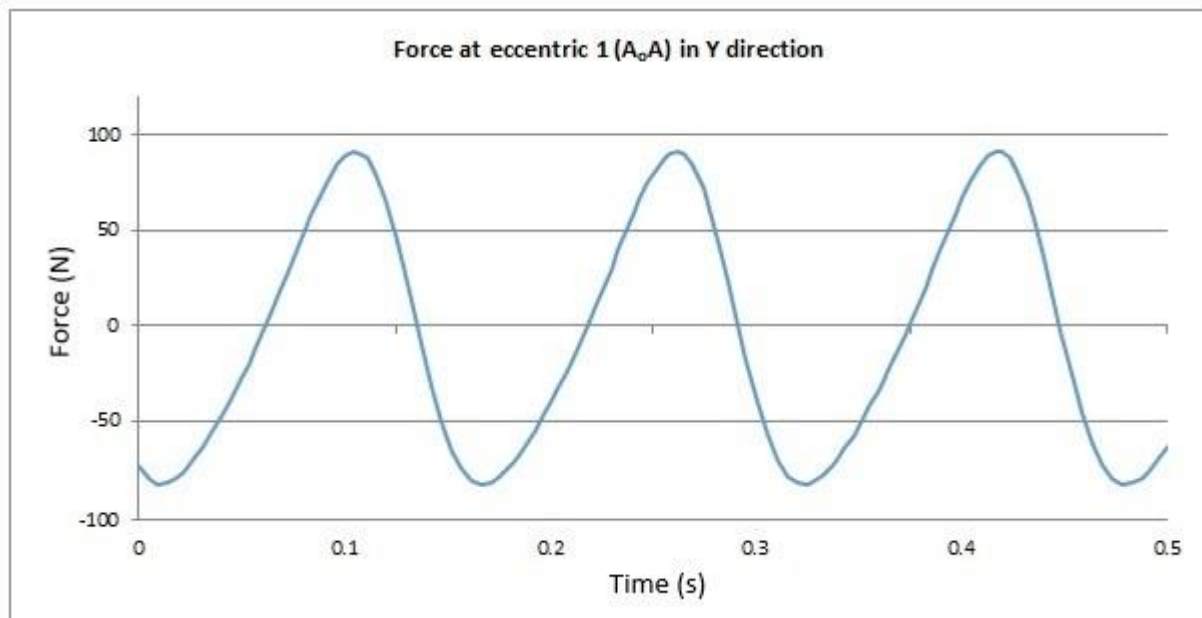


Figure 6.10: Radial force at eccentric 1 (A_0A) in Y direction

6.3.3 Radial force at eccentric 2 (D_oD) in x direction

Dynamic analysis performed and the radial force acting at their joint found. Following chart shows the variation of radial force at the eccentrics D_oD in x direction.

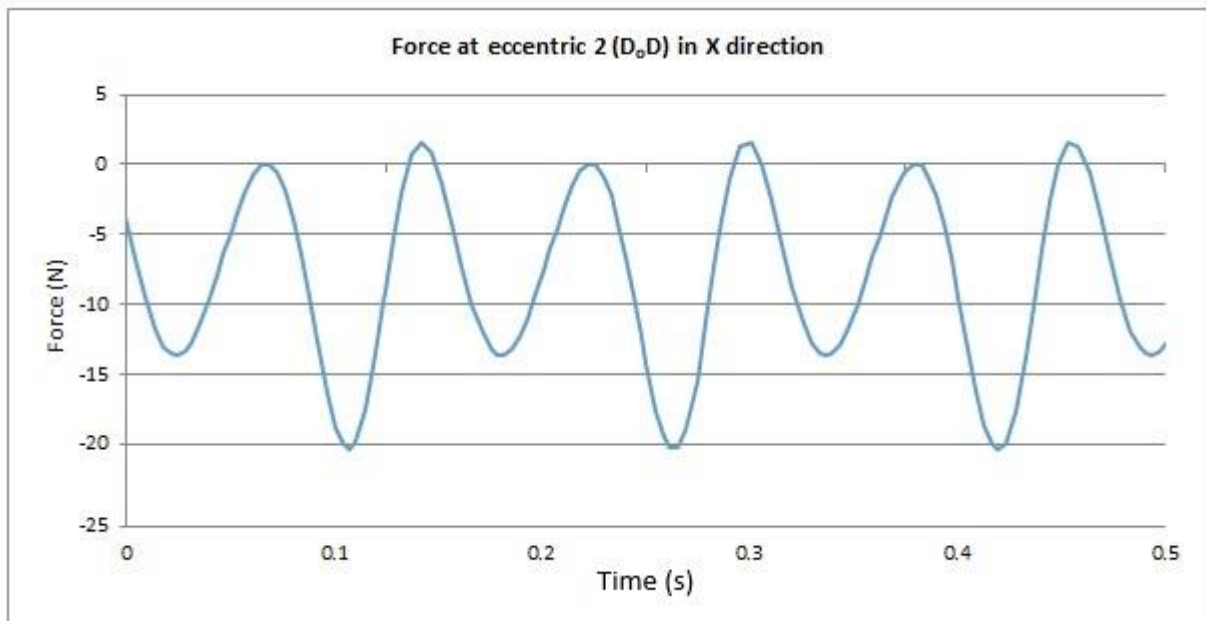


Figure 6.11: Radial force at eccentric 2 (D_oD) in x direction

6.3.4 Radial force at eccentric 2 (D_oD) in y direction

Dynamic analysis performed and the radial force acting at their joint found. Following chart shows the variation of radial force at the eccentrics D_oD in y direction.

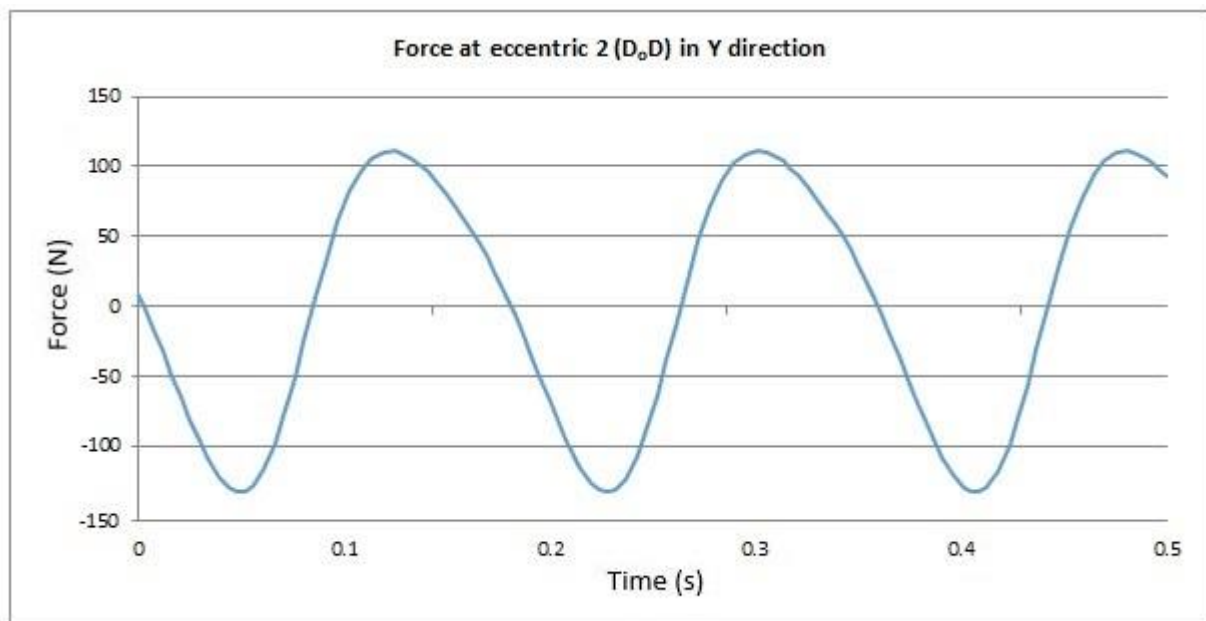


Figure 6.12: Radial force at eccentric 2 (D_oD) in y direction

From the above charts, it is clear that variation of maximum force is minimum between them. Therefore, bearing type used at both places is same. The maximum force acting at their joint from above charts comes out to be 140 N.

6.3.5 Radial force at joint B in x direction

Dynamic analysis performed and the radial force acting at their joint found. Following chart shows the variation of radial force at the joint B in x direction.

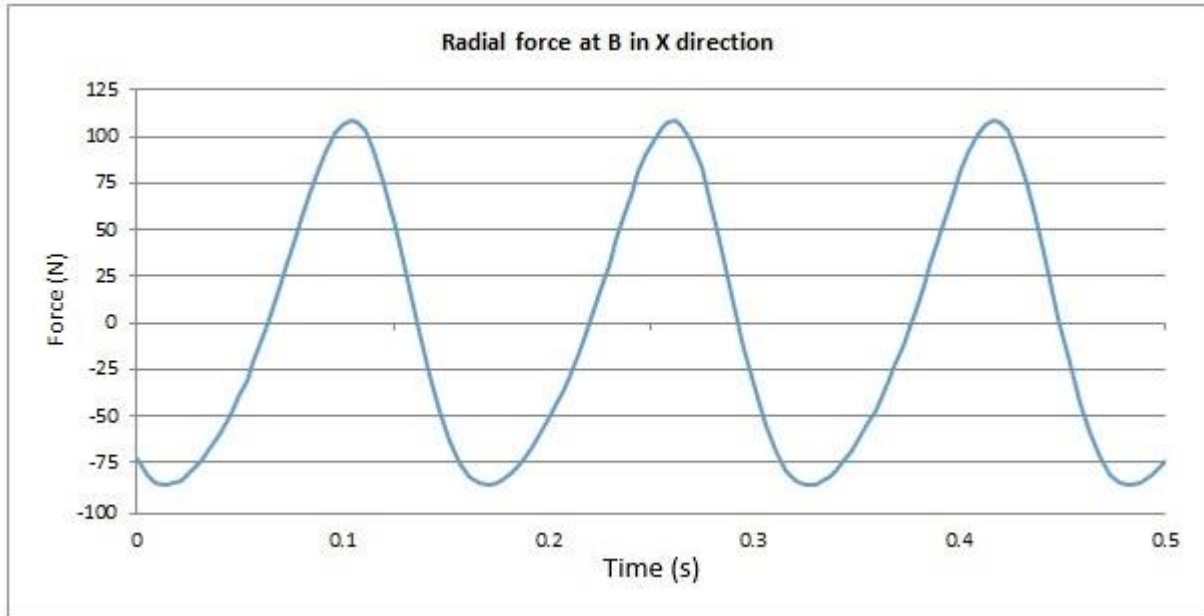


Figure 6.13: Radial force at joint B in x direction

6.3.6 Radial force at joint B in y direction

Dynamic analysis performed and the radial force acting at their joint found. Following chart shows the variation of radial force at the joint B in y direction.

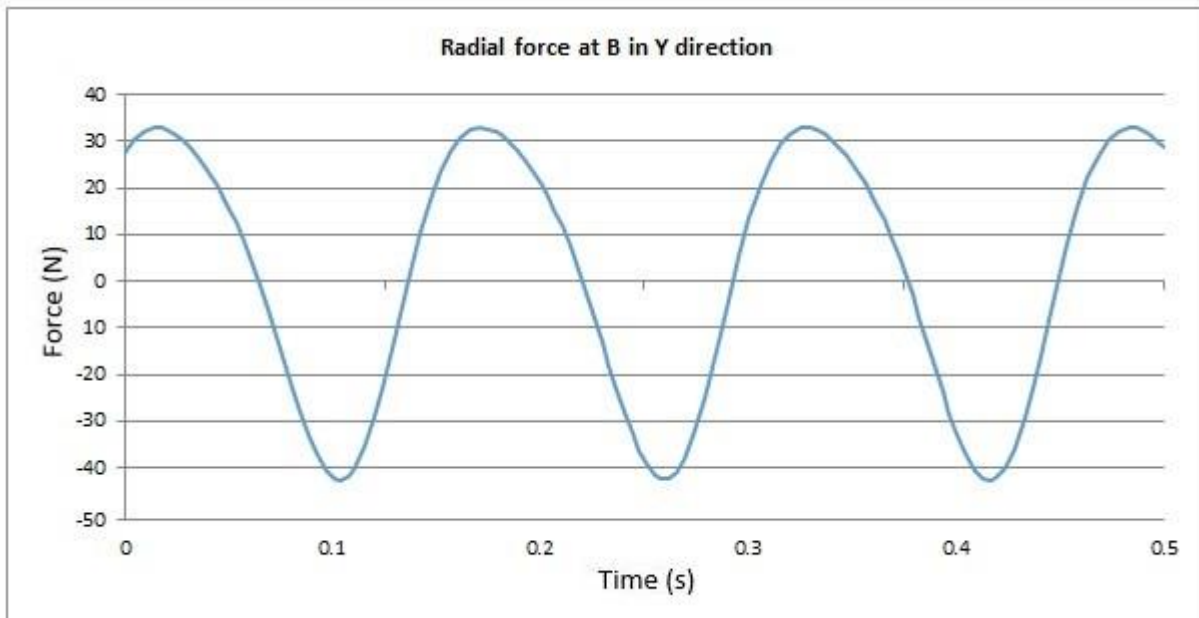


Figure 6.14: Radial force at joint B in y direction

6.3.7 Radial force at joint C in x direction

Dynamic analysis performed and the radial force acting at their joint found. Following chart shows the variation of radial force at the joint C in x direction.

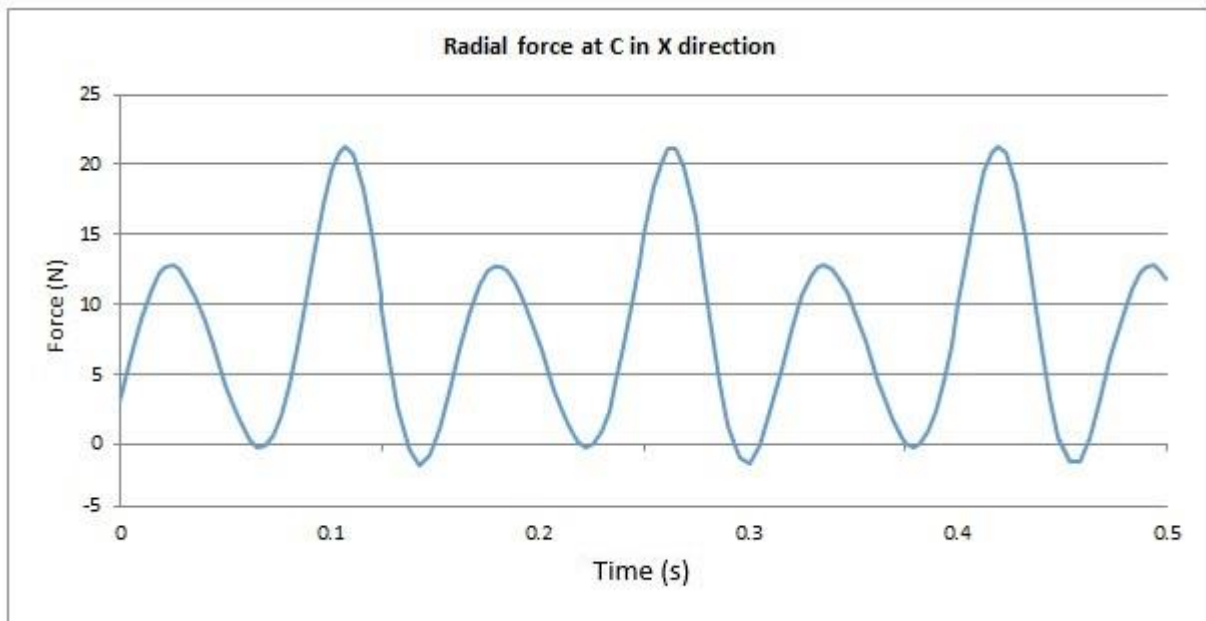


Figure 6.15: Radial force at joint C in x direction

6.3.8 Radial force at joint C in y direction

Dynamic analysis performed and the radial force acting at their joint found. Following chart shows the variation of radial force at the joint C in y direction.

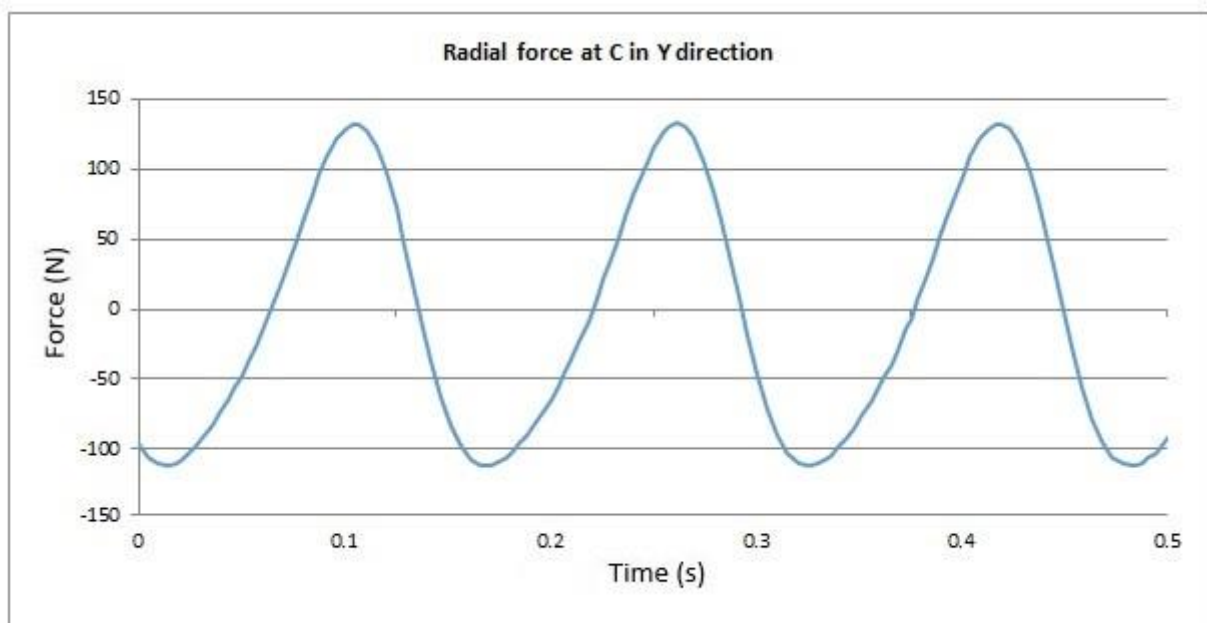


Figure 6.16: Radial force at joint C in y direction

6.3.9 Radial force at joint E in x direction

Dynamic analysis performed and the radial force acting at their joint found. Following chart shows the variation of radial force at the joint E in x direction.

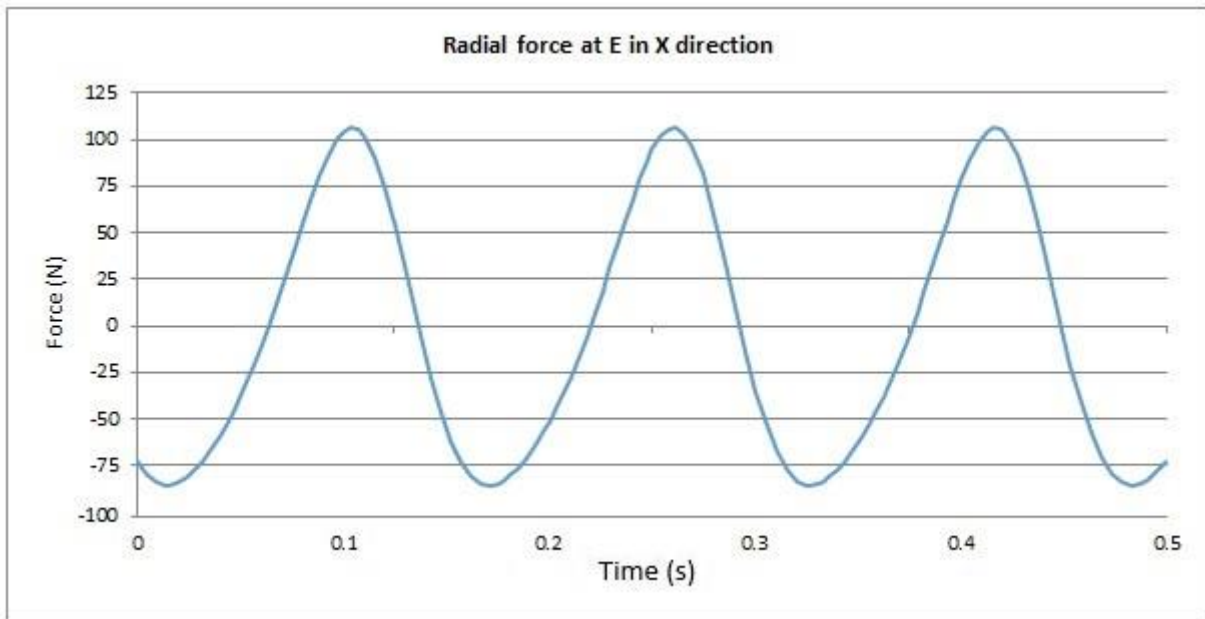


Figure 6.17: Radial force at joint E in x direction

6.3.10 Radial force at joint E in y direction

Dynamic analysis performed and the radial force acting at their joint found. Following chart shows the variation of radial force at the joint E in y direction.

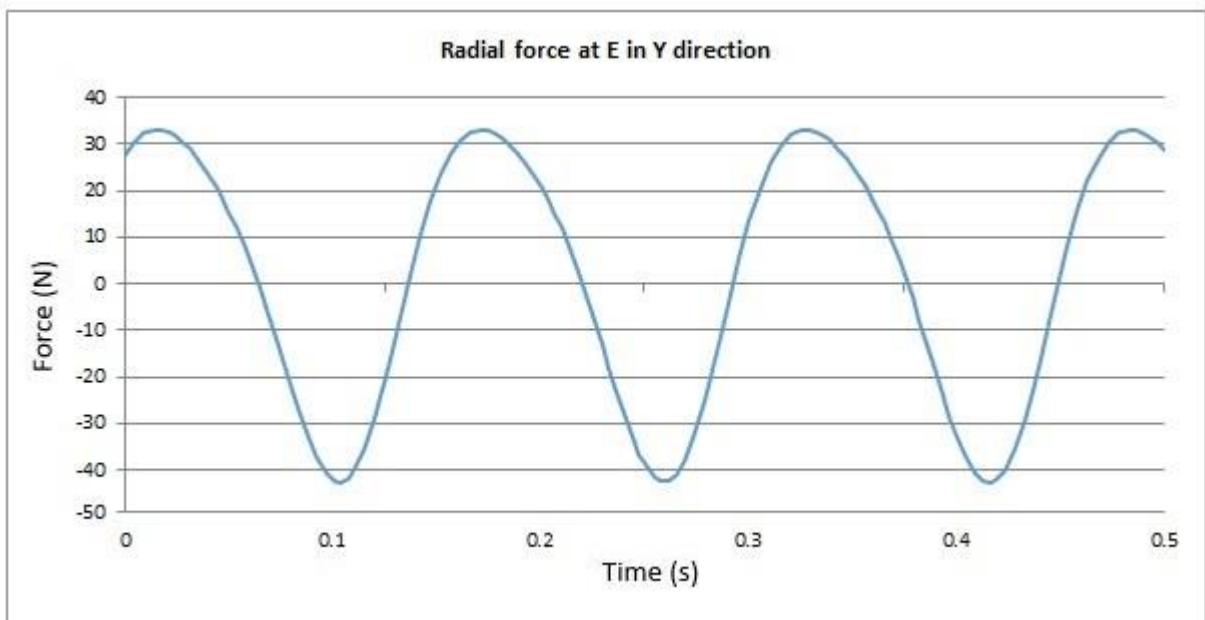


Figure 6.18: Radial force at joint E in y direction

From the above charts, it is clear that variation of maximum force is minimum between them. Therefore, bearing type used at those places is same. The maximum force acting at their joint from above charts comes out to be 140 N.

6.3.11 Type of bearing selected

The following explains the bearings selected for the suitable places.

6.3.11.1 Friction bearing

GBB DP4 flanged bushing chosen for joints at B, C and E. The following picture shows the CAD model of bearing used.

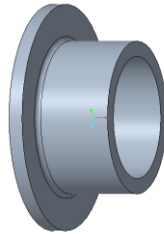


Figure 6.19: GBB flanged plain bearing

The following table shows the load comparison for the respective joints and bearing capacity

Table 6.1: Maximum force at joints

Maximum force comparison at joints	
Radial B	110 N
Radial C	130 N
Radial E	105 N

Table 6.2: Maximum load of friction bearing

Maximum load of bearing	
Static	12.6 KN
Dynamic	7 KN

From the above two tables, it is clear that selected bearing can be used since it has good load capacity. It also has characteristics of good wear capacity and low friction for a wide range of load, temperature and speed in dry conditions.

6.3.11.2 Needle roller bearing

SKF combined needle roller bearings chosen for eccentrics A₀A and D₀D. The following picture shows the CAD model of bearing used.

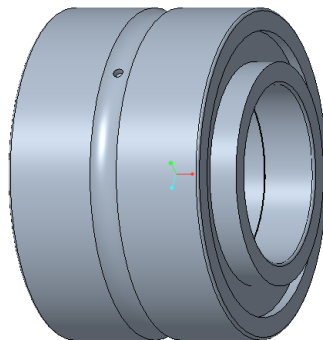


Figure 6.20: SKF needle roller bearing

The following table shows the load comparison for the respective joints and bearing capacity

Table 6.3: Maximum force at eccentrics

Maximum force comparison at eccentrics	
Eccentric A _o A	135 N
Eccentric D _o D	130 N

Table 6.4: Maximum load of needle roller bearing

Maximum load of bearing	
Static	21.6 KN
Dynamic	28 KN

From the above two tables, it is clear that the selected bearing can be used since it has good load capacity. This type of bearing is smaller in diameter in relative to their length hence suitable for miniature linkage. It has ability to withstand both thrust and radial loads. It is also suitable for high speed and dry running conditions.

6.4 Model assembly

The below assembly shows the real model built in the PTC creo parametric system. In the below model, the eccentric shaft 1 was connected as pin revolute joint with ternary link and eccentric shaft 2 was connected as pin revolute joint with connecting rod 1. The power generated from the servomotors makes both the eccentric shafts to rotate. The eccentric shafts 1 & 2 in turn transmits the power to ternary link and connecting rod 1 respectively. The output of ternary link and connecting rod 1 transferred to connecting rod 2, which makes the slider joint to generate the final linear stroke motion. All the above said links such as eccentric shaft 1 & 2, ternary link, connecting rod 1 & 2 and slider joint was constructed using E335 steel.

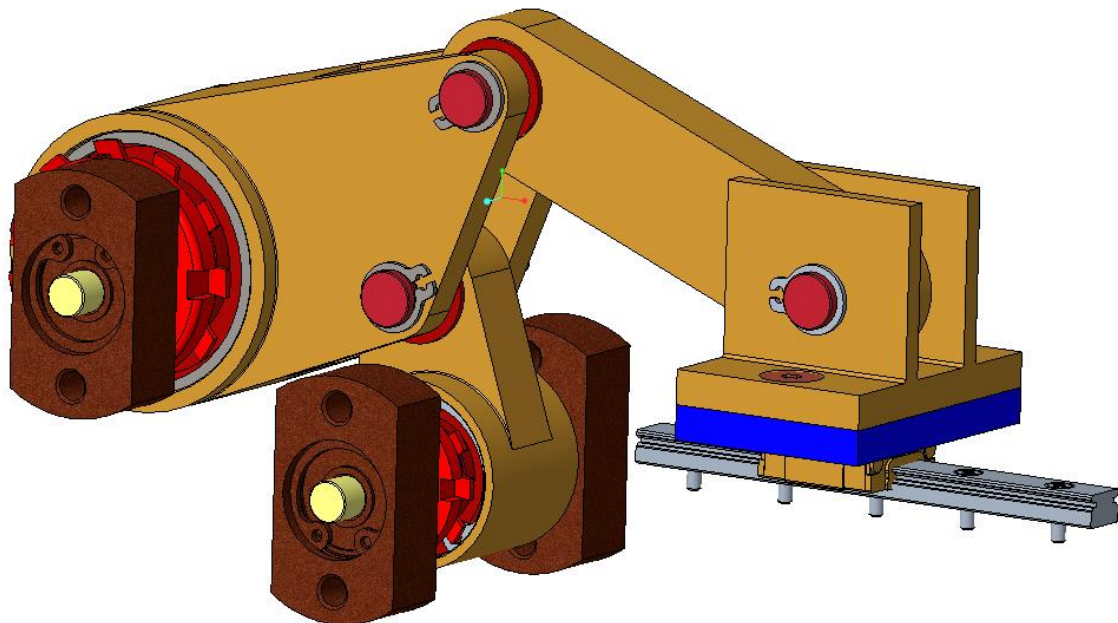


Figure 6.21: Model assembly

6.5 Stress analysis

Stress analysis of the final mechanism done. The individual parts analysed for their stress and displacement behaviour according to the requirement. The following describes the analysis done.

6.5.1 Analysis of eccentric A_oA

Maximum force and its direction acting at eccentric A_oA found. For which, force acting at eccentric A_oA in both x and y direction has to be found separately. The worst case will be the maximum force acting at the eccentric A_oA and this value taken for the stress analysis. The following picture shows the stress and displacement analysis done for the eccentric A_oA.

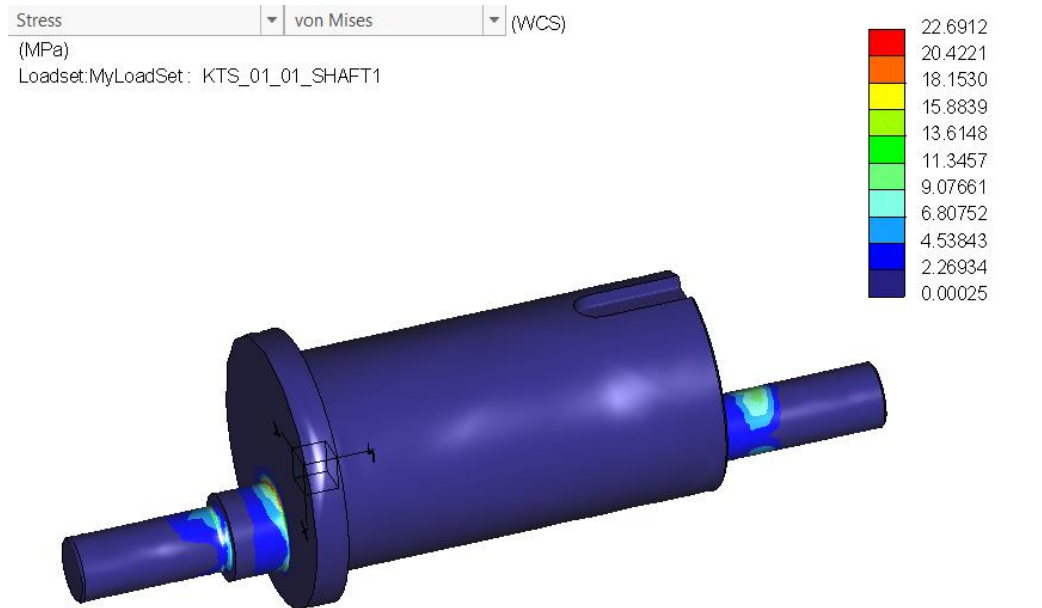


Figure 6.22: Stress analysis of eccentric A_oA

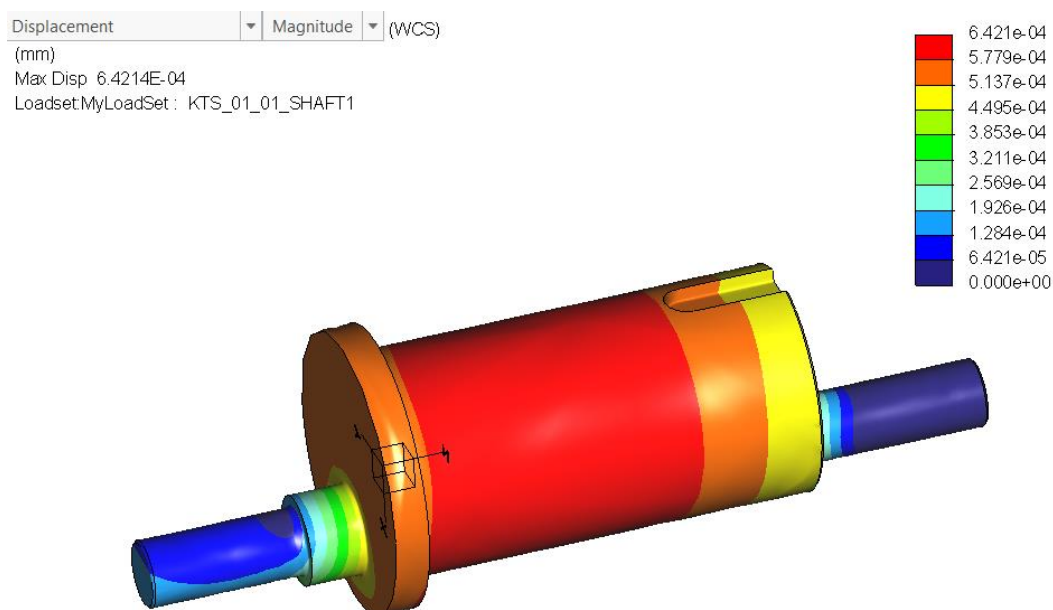


Figure 6.23: Displacement analysis of eccentric A_oA

6.5.2 Analysis of eccentric DoD

Maximum force and its direction acting at eccentric DoD found. For which, force acting at eccentric DoD in both x and y direction has to be found separately. The worst case will be the maximum force acting at the eccentric DoD and this value taken for the stress analysis. The following picture shows the stress and displacement analysis done for the eccentric DoD.

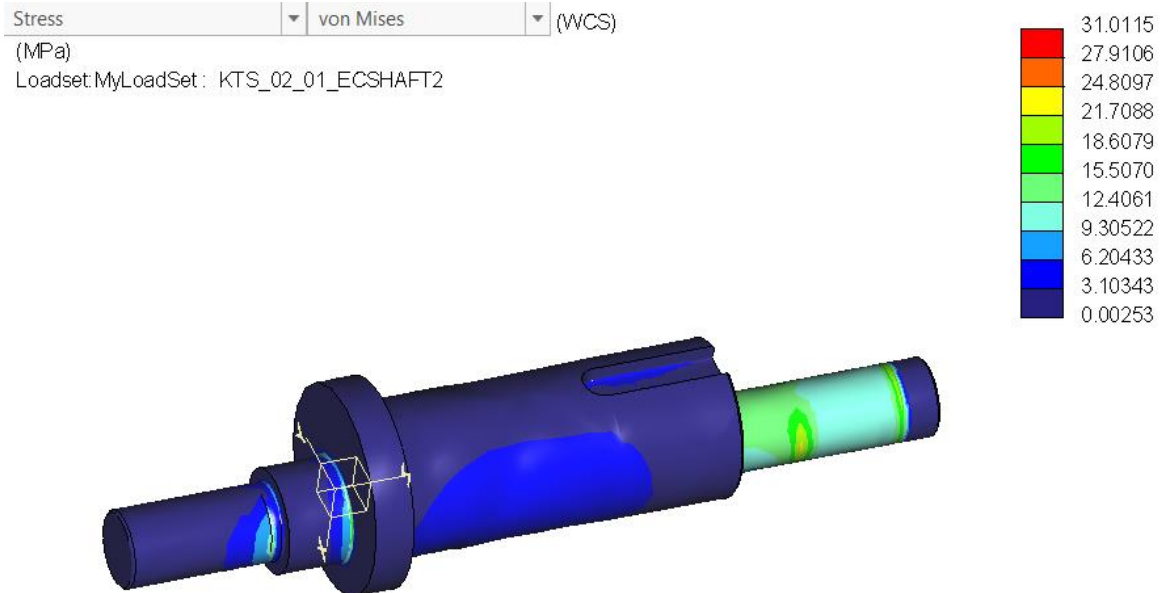


Figure 6.24: Stress analysis of eccentric DoD

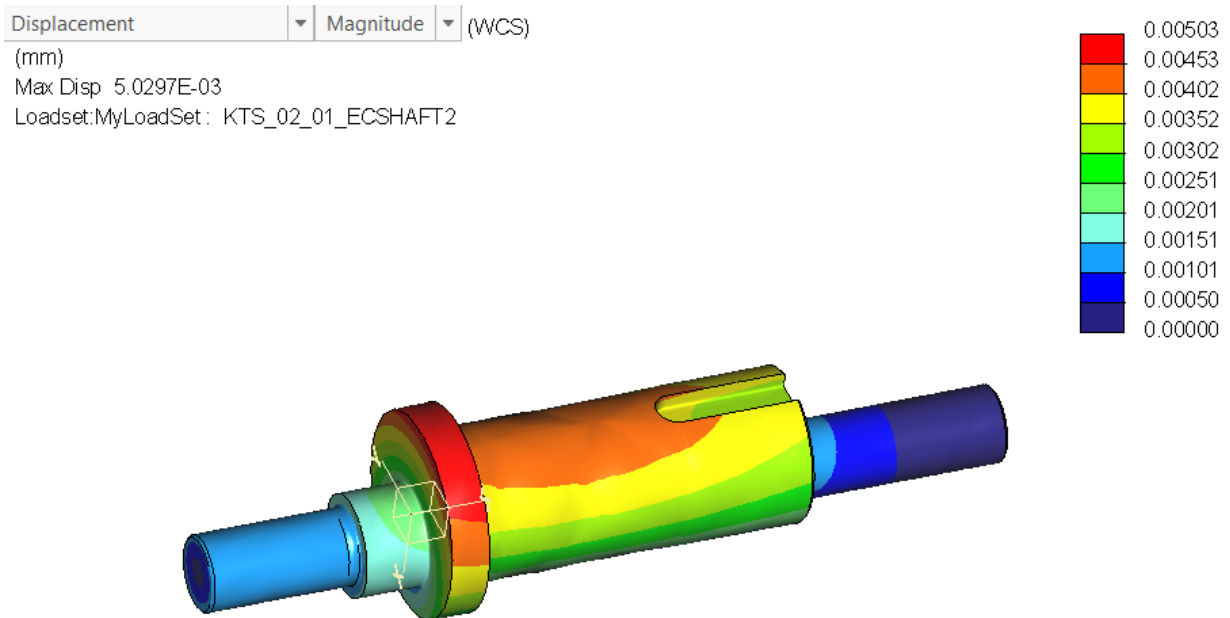


Figure 6.25: Displacement analysis of eccentric DoD

6.5.3 Analysis of link₁

Maximum force and its direction acting at eccentric link₁ found. For which, force acting at eccentric link₁ in both x and y direction has to be found separately. The worst case will be the maximum force acting at the eccentric link₁ and this value taken for the stress analysis. The following picture shows the stress and displacement analysis done for the link₁.

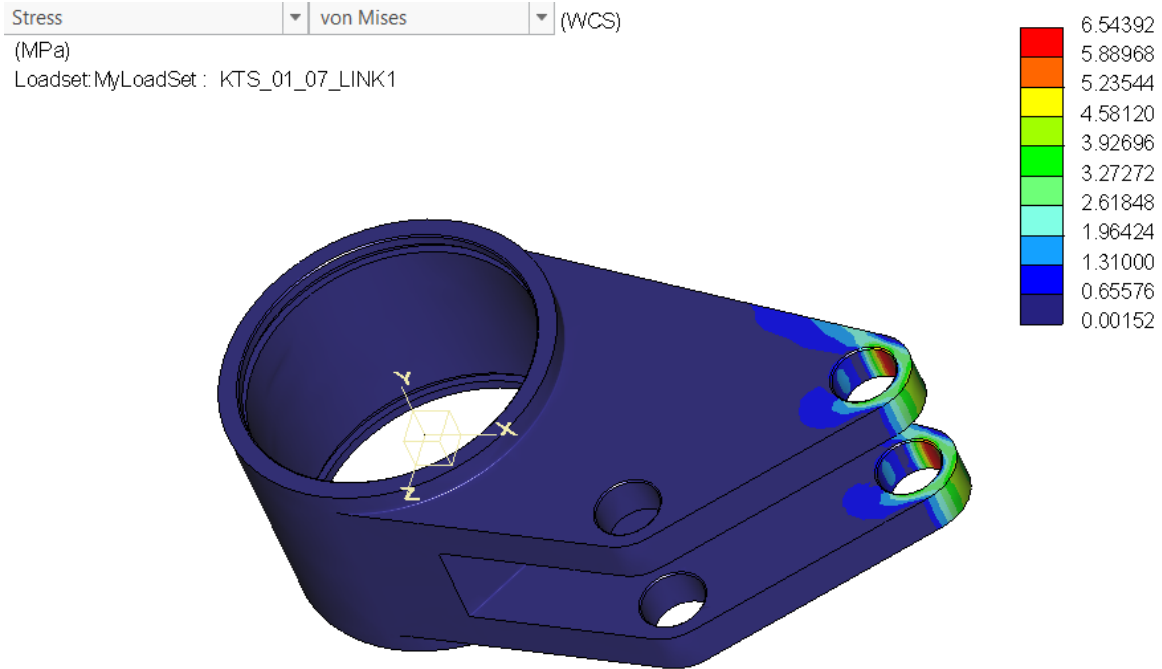


Figure 6.26: Stress analysis of link₁

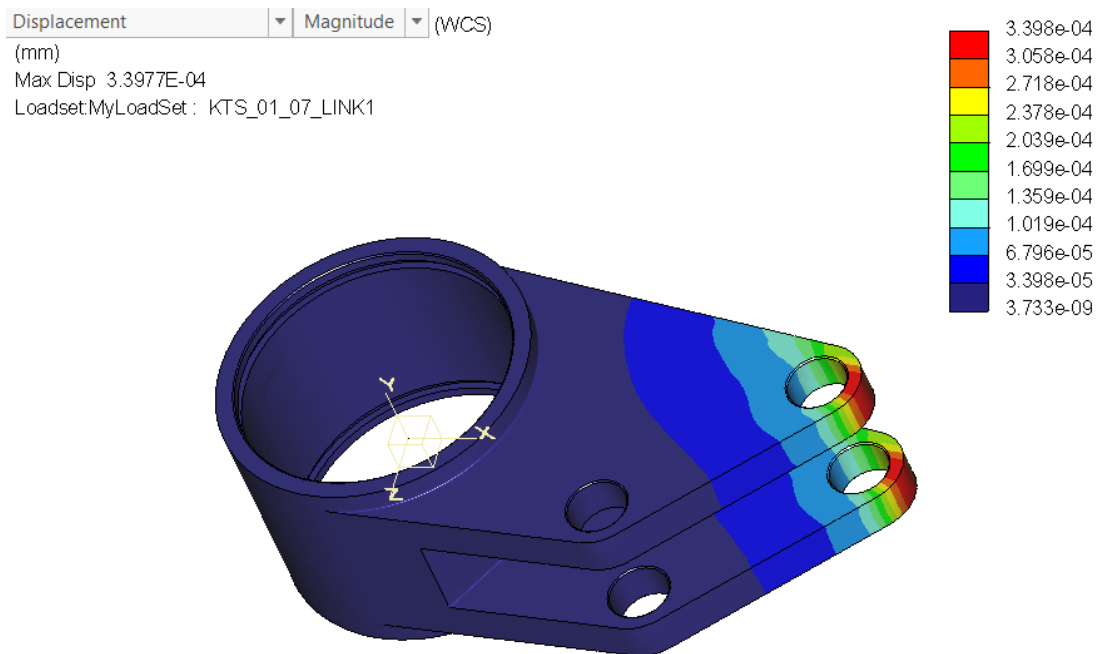


Figure 6.27: Displacement analysis of link₁

6.5.4 Analysis of link₂

Maximum force and its direction acting at eccentric link₂ found. For which, force acting at eccentric link₂ in both x and y direction has to be found separately. The worst case will be the maximum force acting at the eccentric link₂ and this value taken for the stress analysis. The following picture shows the stress and displacement analysis done for the link₂.

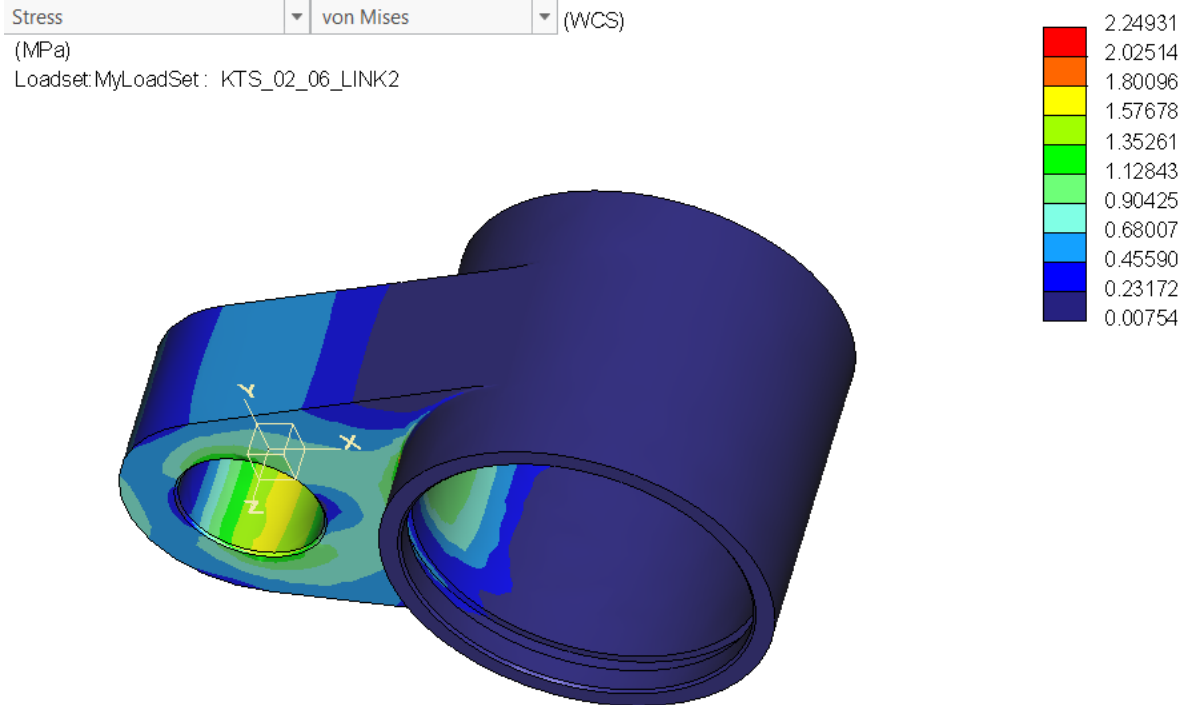


Figure 6.28: Stress analysis of link₂

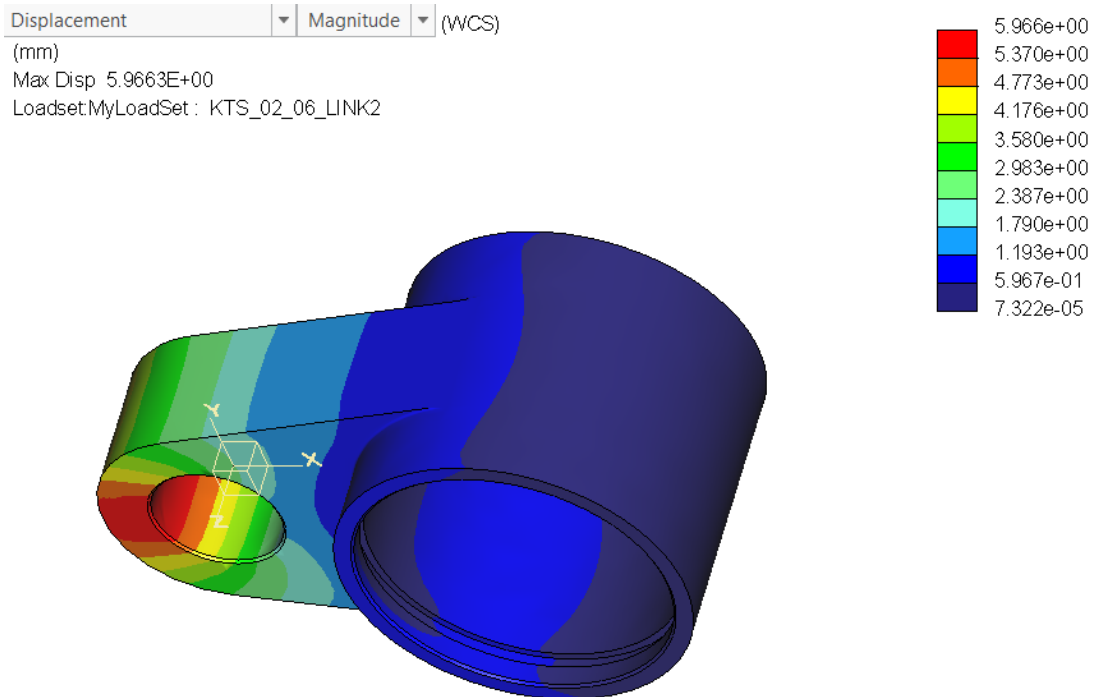


Figure 6.29: Displacement analysis of link₂

6.5.5 Analysis of link₃

Maximum force and its direction acting at eccentric link₃ found. For which, force acting at eccentric link₃ in both x and y direction has to be found separately. The worst case will be the maximum force acting at the eccentric link₃ and this value taken for the stress analysis. The following picture shows the stress and displacement analysis done for the link₃.

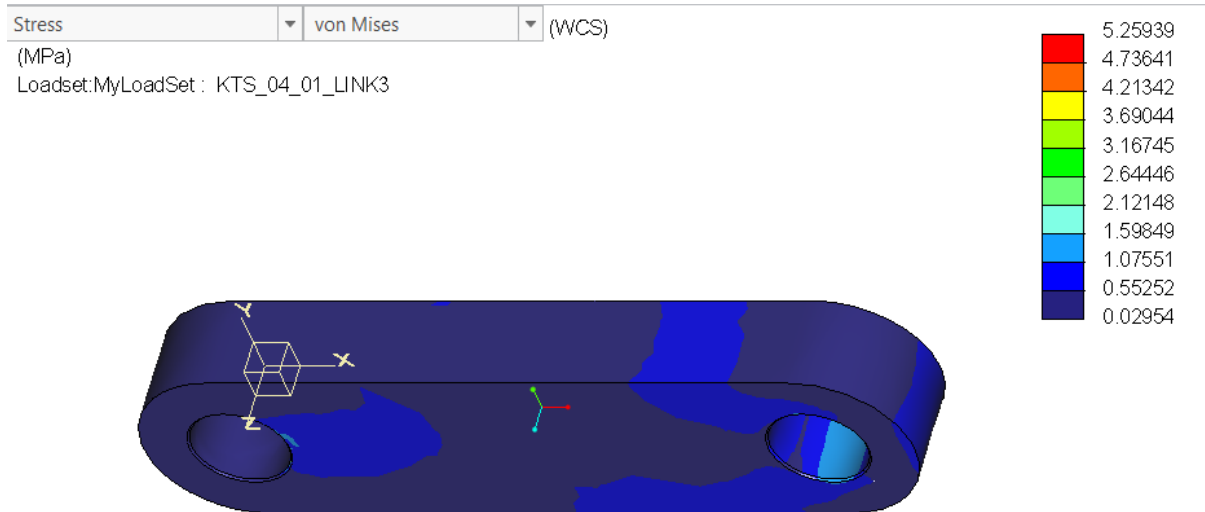


Figure 6.30: Stress analysis of link₃

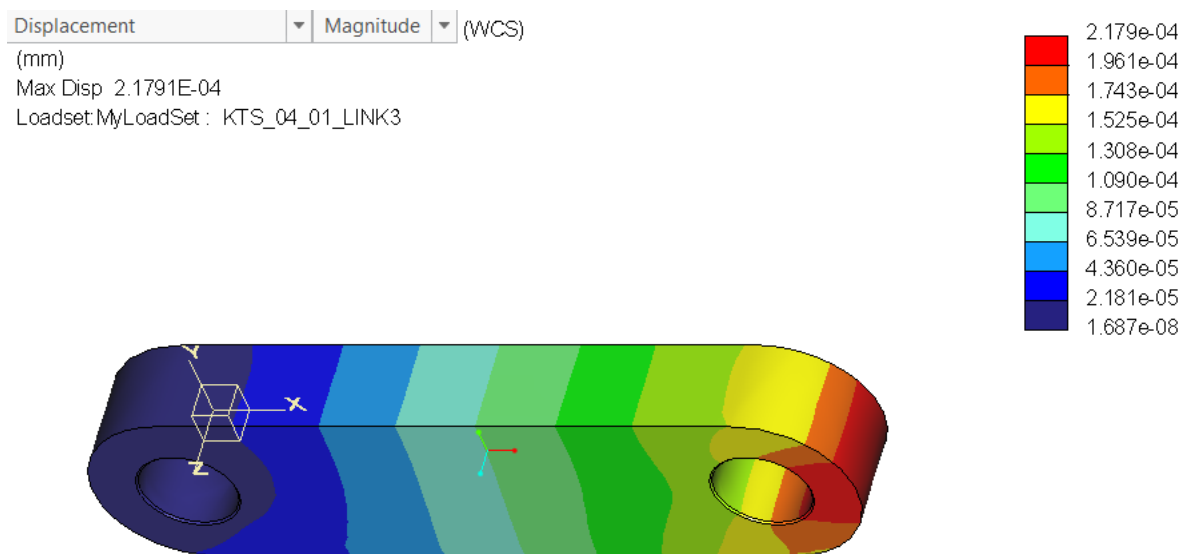


Figure 6.31: Displacement analysis of link₃

7 CONCLUSION

This project aimed to provide a range of stroke variation using single differential mechanism. Previously it required different slider crank mechanism for different length of stroke variation. The solution was combine two crank input from two servomotors into one slider output. For which a differential mechanism designed and analytically calculated the dimension of each link of the mechanism.

For designing the mechanism, many literatures reviewed and research done. From the research and lateral thinking two different variants found one with nine-bar mechanism and one with seven-bar mechanism. Based on the compatibility, production and cost effective, seven bar mechanism declared as chosen variant. In which two variants for seven bar mechanism have proposed and the variant with eccentrics had chosen as final proposal considering better mechanism building.

Analytically dimension of the links of the mechanism have calculated. The calculated dimension used to build the mechanism in the PTC creo parametric system. Modification done using PTC creo parametric mechanism for kinematic analysis so that the required range of stroke variation achieved.

Real model built using the final dimension calculated from the kinematic analysis. Dynamic analysis performed to calculate the forces acting at their joints so that suitable bearing selected. The building of real model completed and all bearing installed. Stress analysis done for all the parts designed.

Working forces are difficult to analyse. Assumption done that maximum forces acting at the joints will be significantly less than the dynamic effects from inertial masses.

The electronically controlled differential mechanism enables efficient and fast change of technological parameters and thus enables automation of the production process with optimized process conditions. Transformation of rotational motion by means of eccentrics is very efficient with low demands on energy consumption. Servomotors perform a one-sided rotary motion only with a change of phase shift. These aspects lead to a reduction in energy intensity and at the same time, this mechanism will enable effective optimization of the production process.

Finally, the project solved the issue and provided a differential mechanism, which used for achieving a range of stroke variation.

8 REFERENCES

1. CHIRONIS, Nicholas P. *Mechanisms & mechanical devices sourcebook*. Fourth Edition. New York: McGraw-Hill, 1991. ISBN ISBN-13: 978-0-07-146761-2.
2. KÜTÜK, M. Erkan a L. Canan DÜLGER. Hybrid Seven-bar Press Mechanism. *Tehnički glasnik* [online]. 2018, **12**(3), 181-187 [cit. 2021-5-6]. ISSN 18485588. Dostupné z: doi:10.31803/tg-20180203202102.
3. G. AMBEKAR, Ashok. *Mechanism and machine theory*. New delhi: Prentice hall of india, 2007. ISBN 978-81-203-3134-1.
4. *MER 312: Dynamics and Kinematics (of Mechanisms) / AT* [online]. New york: Union College Mechanical Engineering, 2010 [cit. 2020-5-6]. Dostupné z: <http://www.engineering.union.edu/~tchakoa/mer312/Lectures/Lecture%202.pdf>
5. Degrees of freedom. *Wikipedia* [online]. online: wikimedia, 2020 [cit. 2020-4-6]. Available from: https://en.wikipedia.org/wiki/Degrees_of_freedom_%28mechanics%29
6. *Geometrical Precision of Mechanism*. Liberec, 2019. Student. Technical university of Liberec.
7. *Transmission angle of mechanism*. Liberec, 2019. Student. Technical university of Liberec.
8. *What Are Bearings? Let's learn about the basic functions of bearings!* [online]. Global: Koyo, 2019 [cit. 2021-5-6]. Dostupné z: <https://koyo.jtekt.co.jp/en/2019/06/column01-01.html>
9. *Design of machine elements*. Third Edition. New delhi: McGraw-hill, 2010. ISBN 978-0-07-061141-2.
10. LI, Hui a Yuping ZHANG. Seven-bar mechanical press with hybrid-driven mechanism for deep drawing; Part 1: kinematics analysis and optimum design. *Journal of Mechanical Science and Technology* [online]. 2010, **24**(11), 2153-2160 [cit. 2020-7-7]. ISSN 1738-494X. Dostupné z: doi:10.1007/s12206-010-0819-0.

LIST OF DRAWINGS

NUMBER	NAME	SIZE
1	KTS_00_00_7BAR	A2
2	KTS_01_00_EC1	A3
3	KTS_01_01_SHAFT	A3
4	KTS_02_00_EC2	A3
5	KTS_02_01_ECSHAFT	A3
6	KTS_03_00_LINK1	A3
7	KTS_01_07_LINK1	A2
8	KTS_02_09_PINSHAFT	A4
9	KTS_04_00_LINK2	A3
10	KTS_02_06_LINK2	A3
11	KTS_05_00_LINK3	A3
12	KTS_04_01_LINK3	A3
13	KTS_03_04_BASEPLATE	A3
14	KTS_03_05_SLIDERJOINT	A3
15	KTS_03_06_PINSLIDER	A4